processes

MDPI

Review

Nirmatrelvir: From Discovery to Modern and Alternative Synthetic Approaches

Michela Galli †, Francesco Migliano †, Valerio Fasano, Alessandra Silvani, Daniele Passarella and Andrea Citarella *

Dipartimento di Chimica, Università degli Studi di Milano, Via Golgi 19, 20133 Milan, Italy; michela.galli2@studenti.unimi.it (M.G.); francesco.migliano@studenti.unimi.it (F.M.); valerio.fasano@unimi.it (V.F.); alessandra.silvani@unimi.it (A.S.); daniele.passarella@unimi.it (D.P.)
* Correspondence: andrea.citarella@unimi.it
† These authors contributed equally to this work.

Abstract: The global urgency in response to the COVID-19 pandemic has catalyzed extensive research into discovering efficacious antiviral compounds against SARS-CoV-2. Among these, Nirmatrelvir (PF-07321332) has emerged as a promising candidate, exhibiting potent antiviral activity by targeting the main protease of SARS-CoV-2, and has been marketed in combination with ritonavir as the first oral treatment for COVID-19 with the name of Paxlovid™. This review outlines the synthetic approaches to Nirmatrelvir, ranging from Pfizer's original method to newer, more sustainable strategies, such as flow chemistry strategies and multicomponent reactions. Each approach's novelty and contributions to yield and purification processes are highlighted. Additionally, the synthesis of key fragments comprising Nirmatrelvir and innovative optimization strategies are discussed.

Keywords: nirmatrelvir; paxlovid; SARS-CoV-2; COVID-19; protease inhibitors; main protease

Citation: Galli, M.; Migliano, F.; Fasano, V.; Silvani, A.; Passarella, D.; Citarella, A. Nirmatrelvir: From Discovery to Modern and Alternative Synthetic Approaches. *Processes* **2024**, *12*, 1242. https://doi.org/10.3390/pr12061242

Academic Editor: Alina Bora

Received: 20 May 2024
Revised: 10 June 2024
Accepted: 14 June 2024
Published: 17 June 2024

1. Introduction

The devastating COVID-19 pandemic has prompted scientists to swiftly focus on finding novel molecules or scaffolds exhibiting antiviral properties, aiding in the mitigation of SARS-CoV-2-induced illness. Academic and industrial researchers have delved into molecules previously advanced in the drug-discovery pipeline, rigorously testing their efficacy against COVID-19. In addition to well-known marketed antiviral drugs, such as remdesivir, favipiravir, and umifenovir, *inter alia*, scientists' attention focused on PF-00835231, which is endowed with strong antiviral efficacy against SARS-CoV-1 [1]. To establish a structure–activity relationship (SAR) for PF-00835231, researchers synthesized analogs by modifying the constituent amino acids with six notable fragments. Among these, the most promising analog, PF-07321332 (Nirmatrelvir), received FDA approval in December 2021 as part of an antiviral combination pill for home use, aimed at preventing severe illness in patients infected with COVID-19 [2]. Nirmatrelvir exerts its antiviral activity via the covalent inhibition of the main protease of SARS-CoV-2 (SARS-CoV-2 M^{pro}) [3]. However, its efficacy is limited when administered alone in vivo, due to rapid metabolism by the CYP3A4 enzyme. To overcome this limitation, Nirmatrelvir found suitability for therapeutic application in combination with ritonavir, initially formulated as an HIV protease inhibitor. Ritonavir effectively enhances the bioavailability of Nirmatrelvir by inhibiting CYP3A4. This synergistic combination, developed by Pfizer, is marketed as Paxlovid™ [4]. As stated by real-world data, Paxlovid™ showed proven efficacy in preventing COVID-19 progression among high-risk individuals, significantly reducing the need for hospitalization and supplementary oxygen administration [5,6]. However,

ongoing monitoring and research are essential to better understand its long-term efficacy and potential resistance issues in diverse patient populations.

This review will provide the reader with an overview of the most significant synthetic approaches to Nirmatrelvir, starting from the original one developed by Pfizer, and then incorporating new, more sustainable synthetic approaches, such as flow chemistry or multicomponent reactions, taken from the recent literature. The novelty of the methods will be thoroughly explored, emphasizing the distinctive contributions that each step imparts to the final yields or purification processes. Moreover, the syntheses of the main fragments that constitutes Nirmatrelvir and the innovative strategies that facilitated their optimization will also be briefly discussed individually.

2. Development of Nirmatrelvir

Following the global emergency caused by the spread of SARS-CoV-2, leading pharmaceutical companies have embarked on efforts to research efficacious vaccines to contain the virus's spread among humans and valuable therapies to mitigate the severity of COVID-19 infections. While a wide range of vaccines has been produced during the pandemic, only one orally administered drug has been approved by the FDA and made available on the market for the treatment of severe forms of COVID-19. Paxlovid consists of the combination of two medications: Nirmatrelvir, which inhibits the viral replication process, and ritonavir, which helps boost the levels of Nirmatrelvir in the body. Paxlovid is administered orally and has been authorized for emergency use in several countries as a treatment for individuals with mild to moderate COVID-19 symptoms, who are at high risk of progressing to severe illness [7]. This medication emerged when vaccination campaigns were underway in many countries, while some others had already achieved high vaccination rates. This timing was not coincidental as, during this period, despite vaccines showing beneficial effects on reducing hospitalizations and mortality rates, there was significant concern about potential virus mutations that could diminish vaccine efficacy. Consequently, there was a pressing urgency for orally available, cost-effective antiviral treatments to administer, aiming to minimize COVID-19-associated deaths.

Before Paxlovid marketing, the FDA had repurposed several other therapeutics for treating COVID-19 infection. One such example is the RdRp inhibitor remdesivir, which is intravenously administered to COVID-19-infected hospitalized adults and children. Several challenges were associated with this medication, including its low stability in the blood and limited half-life (necessitating continuous administration). Molnupiravir, another RdRp inhibitor, has obtained full regulatory approval in the UK. The advantage in this case relies in its oral bioavailability. Within this context, there was a growing demand for orally bioavailable therapeutics against COVID-19, which finally led to the development and approval of Nirmatrelvir.

2.1. Target Validation: SARS-CoV-2 M^{pro}

Nirmatrelvir is a potent inhibitor of SARS-CoV-2 M^{pro}, thereby blocking viral replication and strongly reducing the severity of COVID-19 infection [8,9]. M^{pro} plays a crucial role in the viral replication cycle by processing the polyproteins translated from the viral RNA [10]. The protease cleaves these polyproteins at specific sites to generate active viral proteins essential for RNA replication and transcription. A selective inhibition of M^{pro} effectively alters the synthesis of such vital components, thereby disrupting the virus's capability to replicate and spread. Due to its indispensable role and the absence of a human counterpart with similar cleavage specificity, M^{pro} becomes an ideal target for antiviral drug development [11]. This enzyme's conservation across coronaviruses further enhances its appeal, offering potential broad-spectrum antiviral activity. Consequently, inhibitors of M^{pro}, such as Nirmatrelvir, hold significant promise in treating COVID-19 and possibly other coronavirus-related diseases. Figure 1 depicts the main structural features of Nirmatrelvir. The terminal -CN functional group is the key component of the entire molecule as it essentially represents its "electrophilic warhead", which undergoes a

covalent reaction with the reactive Cys145 thiol group of the target. Meanwhile, the remaining portion of the molecule, emulating the natural recognition sequence of M^{pro}, specifically the tripeptide Val-Leu-Gln, ensures Nirmatrelvir's snug accommodation within the enzyme's active site, where it establishes supplementary interactions. The recognition motif consists of a P1 unit formed by a Gln analog featuring a cyclic (γ-lactam) side chain and this modification makes noteworthy advantages because the native Gln's amide group can intramolecularly react with certain types of warheads, leading to inhibitor inefficacy. The cyclic moiety offers greater rigidity compared to the native Gln side chain, which may enhance binding to the target enzyme. Additionally, converting Gln into a cyclic derivative improved synthetic accessibility. The P2 group is made of a dimethylcyclopropyl proline (DMCP) moiety, serving as a leucine analog that predominantly interacts with the enzyme through lipophilic interactions. Finally, the P3 residue is a tertiary leucine, mimicking valine protected at the N-terminal with a trifluoroacetyl group. A covalent reversible interaction occurs between Nirmatrelvir and M^{pro} thanks to the presence of the reactive electrophilic warhead. The P1' nitrile group establishes a thioimidate bond with the Cys145 thiol functional group of M^{pro} via a Pinner-like mechanism. Even if -CN is a less reactive warhead in comparison to aldehydes or Michael's acceptors, it offers enhanced selectivity and metabolic stability. Moreover, the thioimidate adduct is stabilized within the binding pocket thanks to supplementary interactions, strengthening the affinity. Finally, given that the thiol group of Cys145 is crucial for catalyzing the hydrolysis of peptide bonds, the enzyme's functionality is interrupted.

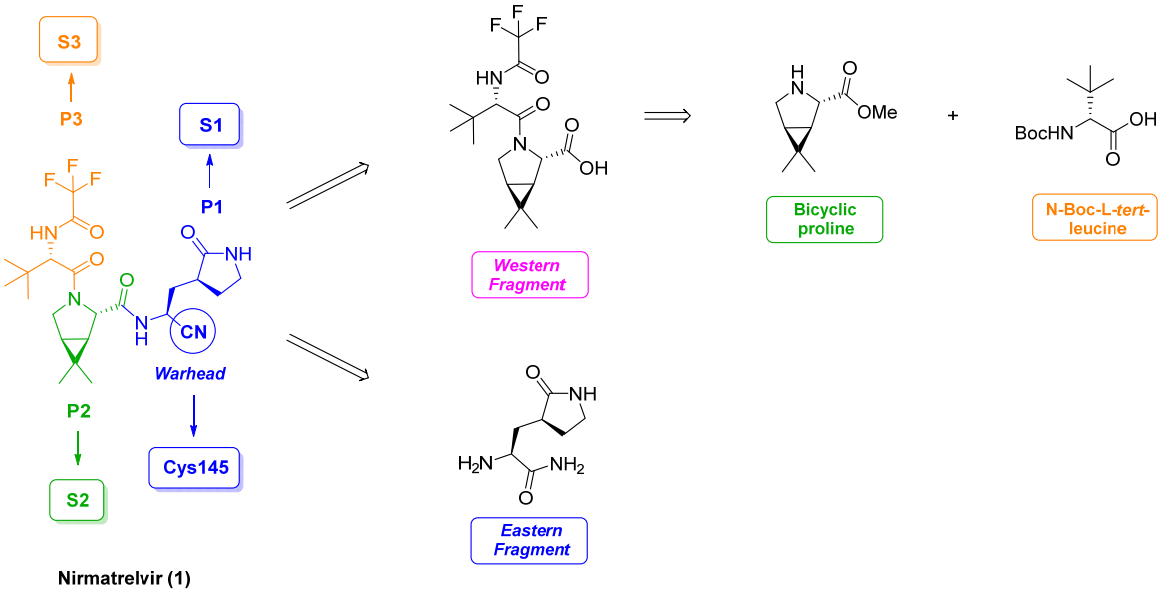

Figure 1. Main structural components of Nirmatrelvir.

2.2. Lead Discovery and Optimization

The discovery and development of Nirmatrelvir commenced with two hit compounds previously synthesized by Pfizer to counter the SARS-CoV infection: PF-00835231 (referred to as compound **2** in Figure 2), an α-hydroxy ketone-based peptidomimetic, and its corresponding phosphate prodrug, PF-07304814 (referred to as compound **3** in Figure 2).

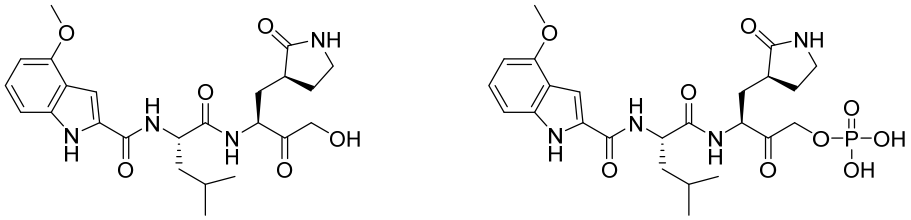

2 **3**

Figure 2. Structure of PF-00835231 and its phosphate prodrug PF-07304814.

Compounds **2** and **3** were selected for in vitro and in vivo evaluations against SARS-CoV-2 M^{pro} and SARS-CoV-2-infected cells and they showed promising results, in particular, PF-00835231 (**2**) exhibited high inhibitory potency ($K_i = 4 \pm 0.3$ nM) and good antiviral activity ($EC_{50} = 231$ nM). One noteworthy aspect of these two hit compounds was the presence of a P1 γ-lactam moiety, which mimics the native substrate's Gln and serves as a recognition motif for the S1 pocket. The challenge associated with using free glutamine was the potential intramolecular reaction of the side-chain amino group with the electrophilic warhead, resulting in a cyclized inactive product. Indeed, this issue was circumvented by employing lactam functionality, which not only prevents such a side reaction, but also imparts rigidity leading to a reduced loss of conformational entropy upon binding to the target [12]. Despite their activity against SARS-CoV-2 M^{pro}, the "first generation" of M^{pro} inhibitors showed poor oral bioavailability, which was in contrast with the aim of Pfizer's chemists to develop an antiviral oral drug to treat COVID-19 at the first stage of viral infection. Hence, Owen et al. designed a library of analogs of PF-00835231 (**2**) with the aim of improving the pharmacokinetic properties (Figure 3) [13]. In particular, the focus was on decreasing the number of H-bond donor (HBD) groups to increase gut absorption without affecting drug target recognition or the potency of the drug. The first modification involved the electrophilic warhead, replacing the α-hydroxy ketone moiety with two new functional groups, a benzothiazole-7-yl ketone and a nitrile group, both missing HBD groups. Nitrile derivate **4** showed enhanced oral absorption in rats but a lower antiviral and inhibitory activity with respect to PF-00835231 (**2**). Further modifications focused on the P2 leucine moiety, which was replaced with a cyclic modified proline moiety able to fit into the S2 pocket. This fragment was also present in serine protease inhibitor Boceprevir: the X-ray crystal structure of SARS-CoV-2 M^{pro} in a complex with Boceprevir provided a rational structural basis for the incorporation of such a moiety [14]. This modification in combination with the introduction of the benzothiazole-7-yl-ketone warhead produced compound **5**, whose permeability was increased but activity decreased, with respect to that of compound **2**. Therefore, to enhance potency, subsequent investigations revealed the necessity for a substituent in the P3 position that could more effectively occupy the S3 subsite. The indole moiety was then replaced by both a methanesulfonamide and a trifluoroacetamide functionality in **6** and **7**. These compounds showed comparable potency, but **7** proved to be a better antiviral candidate due to its higher antiviral activity and oral absorption in rats and monkeys. The combination of a nitrile warhead with the trifluoroacetamide moiety led to the identification of Nirmatrelvir (**1**) as a novel clinical candidate. The nitrile warhead was selected above the benzothiazole-7-yl-ketone moiety due to some particular features, including the perceived ability to more easily scale-up, better solubility, and a reduced likelihood of epimerization at the stereocenter at the P1 position.

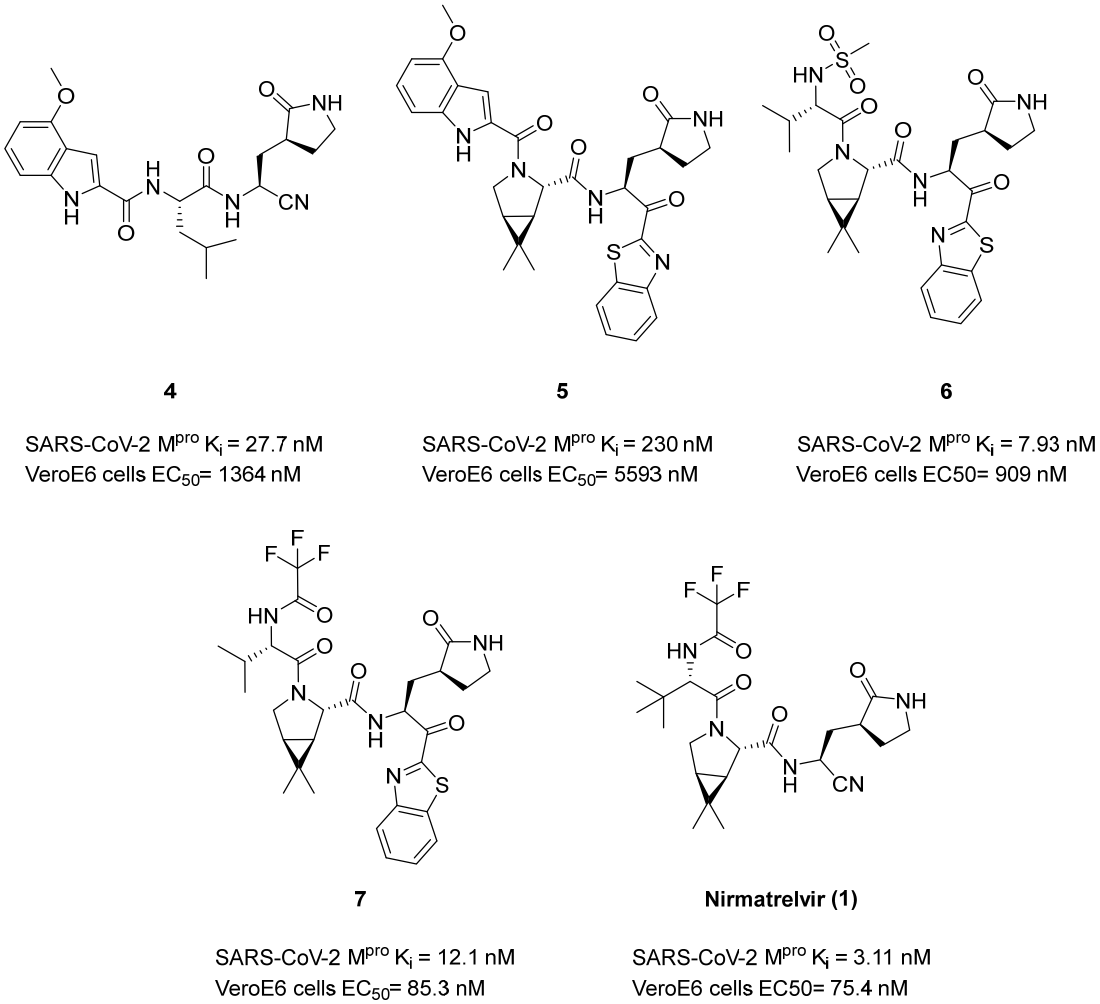

Figure 3. Analog compounds derived from PF-00835231.

Nitrile is an established warhead for targeting serine and cysteine proteases [15]. In fact, the nitrile warhead has previously been explored as a reactive group in many FDA-approved drugs [16]. The electron-poor carbon of the nitrile group is able to undergo a nucleophilic attack from the thiol group of Cys, thus affording a reversible covalent thioimidate adduct. The introduction of the nitrile group instead of the HBD group of the α-hydroxymethyl ketone covalent warhead in **2** led to improved oral bioavability. Table 1 shows all the advantages and disadvantages of each Nirmatrelvir precursor that led the drug development process.

Table 1. Summary of the advantages and disadvantages of each Nirmatrelvir precursor that led the drug development process.

Compound	Advantages	Disadvantages
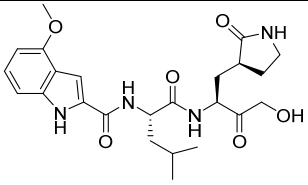 **2**	High inhibitory potency Good antiviral activity	Low oral bioavailability
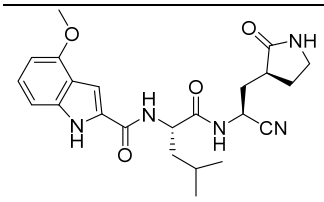 **4**	Lower number of H-bond donors Nitrile warhead enhances oral absorption in rats	Antiviral and inhibitory activities lower than **2**
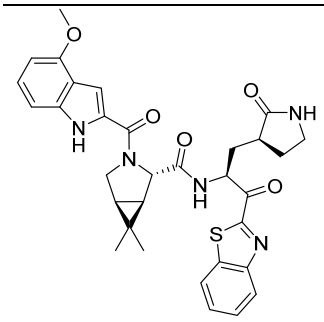 **5**	Benzothiazole-7-yl ketone warhead increases permeability Replacement of leucine with modified proline allows a better fit into the S2 subsite	Antiviral and inhibitory activities lower than **2** and **4**
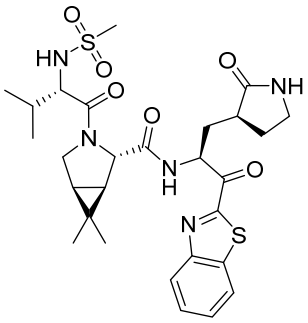 **6**	Replacement of indole with methanesulfonamide allows a better fit into the S3 subsite Antiviral and inhibitory activities higher than **4** and **5**	Antiviral and inhibitory activities lower than **2** Oral absorption in rats and monkeys lower than **7**

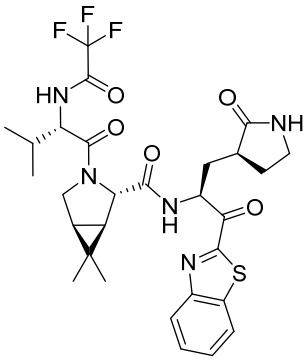 **7**	Replacement of indole with trifluoroacetamide allows a better fit into the S3 subsite Antiviral and inhibitory activities higher than **4** and **5** Oral absorption in rats and monkeys higher than **6**	Antiviral and inhibitory activities lower than **2**
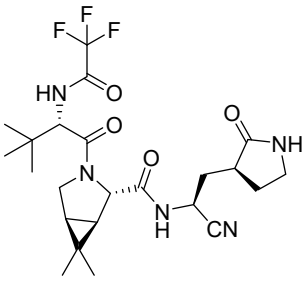 **Nirmatrelvir (1)**	Combination of nitrile warhead, modified proline at P2 position, and trifluoroacetamide at P3 position provides antiviral and inhibitory activities higher than **2** Oral bioavailability higher than all precursors	

3. Synthetic Approaches to Nirmatrelvir

3.1. Pfizer's Synthesis

The original Nirmatrelvir synthesis developed by Pfizer is reported in the patent US11,351,149. The document, filled on 5 August 2021 and published as the PCT application WO2021/250648, presents several examples of the synthesis of Nirmatrelvir [17]. In particular, the procedure described in Scheme 1 allows us to adapt Nirmatrelvir's synthesis also on a larger multigram scale. The synthetic route starts with the bicyclic pyrrolidine derivative **8**, which is reacted with Boc-protected L-tert-leucine **9** in a Hexafluorophosphate Azabenzotriazole Tetramethyl Uronium (HATU)/N,N-Diisopropylethylamine (DIPEA)-mediated amide coupling in DMF to afford **10** in a 50% yield after column chromatography purification. The methyl ester is hydrolyzed in basic conditions to afford **11**. After Boc-deprotection, the reaction of **12·HCl** with ethyl trifluoroacetate produces intermediate **13** in a quantitative yield. The latter reacts with hydrochloric salt **14·HCl**, in the presence of 2-Hydroxypyridine-N-oxide (HOPO) and N-(3-dimetilaminopropil)-N′-etil-carbodiimide crystalline (EDCI·HCl) in DMF, providing **15** in a 84% yield. Primary amide **15** is finally dehydrated with the Burgess reagent to furnish the target Nirmatrelvir (**1**) in an 81% yield. In a recent paper, the possibility of using isobutyl acetate as a solvent to obtain key intermediate **15** as a solvate with higher purity in comparison to its production with other existing synthetic methods is shown [18].

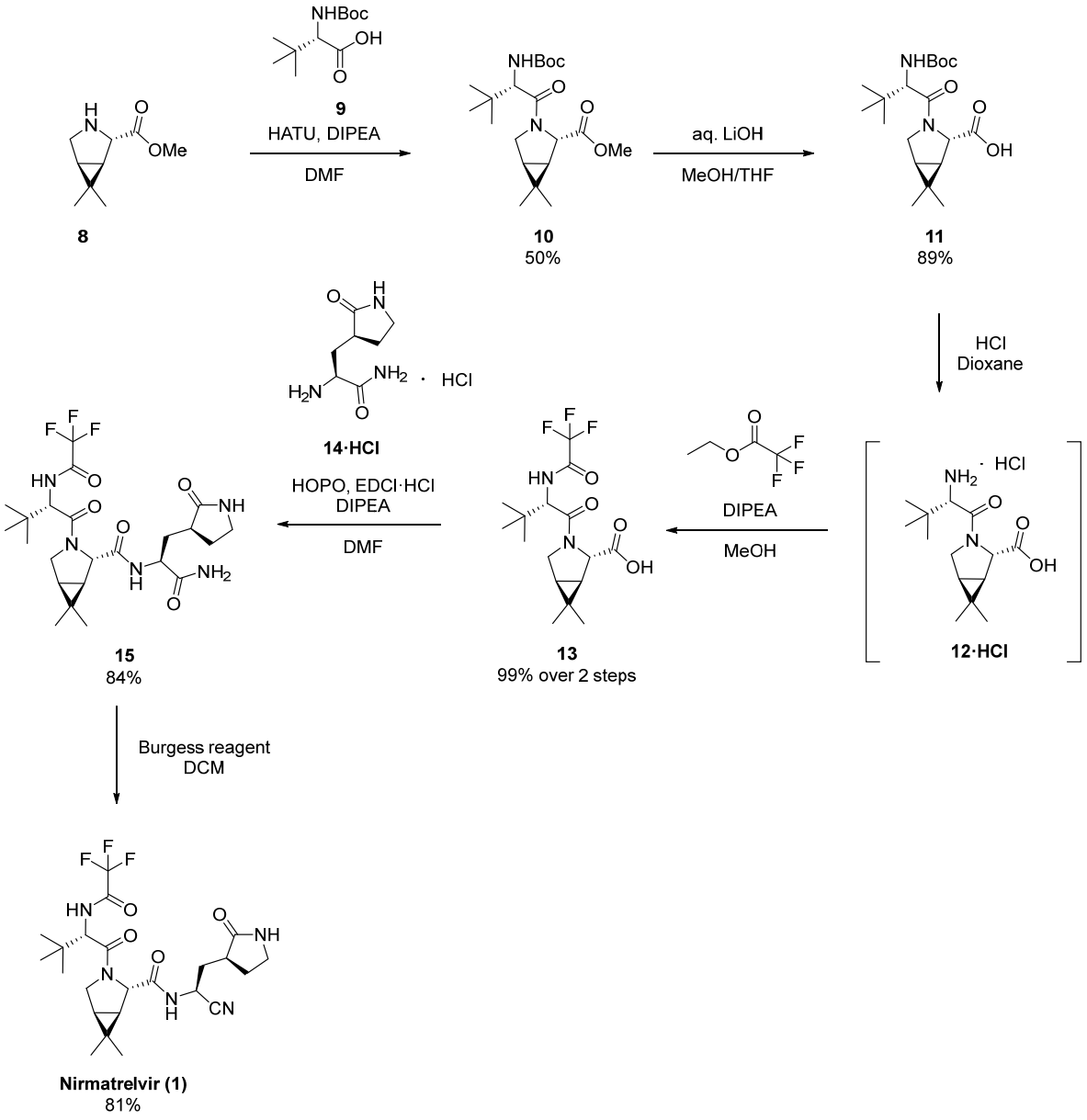

Scheme 1. Patented synthesis of Nirmatrelvir; HATU = Hexafluorophosphate Azabenzotriazole Tetramethyl Uronium, DIPEA = N,N-Diisopropylethylamine, HOPO = 2-Hydroxypyridine-N-oxide, EDCI·HCl = N-(3-dimetilaminopropil)-N′-etilcarbodiimide hydrocloride salt, MeOH = Methanol, DMF = N,N-Dimethylformamide, and DCM = Dichloromethane.

3.2. Structural Components of Nirmatrelvir

Based on the structural analysis, the chemical structure of Nirmatrelvir is considered a peptidomimetic composed of two main fragments, termed the "western fragment" and "eastern fragment", linked via an amide bond (Figure 4). The western fragment comprises a bicyclic proline residue connected to an L-tert-leucine capped with a trifluoroacetyl group, while the eastern fragment consists of a γ-lactam analog of Gln, bearing the terminal electrophilic warhead. Algera et al. discussed the development of the first ever commercial process of Nirmatrelvir, describing the difficulties and challenges due to the extremely accelerated timeline that was needed to face the emergency [19–21]. This paragraph will highlight the strategies for the construction of both fragments, analyzing how

the main synthetic challenges have been approached to obtain to the most effective chemical conditions.

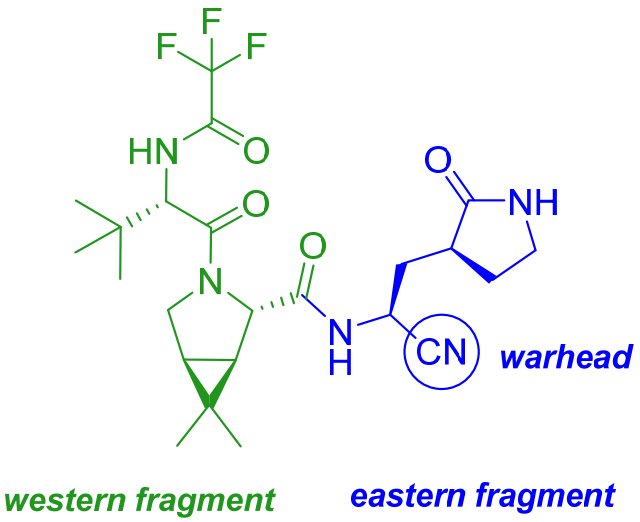

Nirmatrelvir (1)

Figure 4. Structure of Nirmatrelvir with the key fragments and the warhead highlighted.

3.2.1. Synthesis of the Bicyclic [3.1.0] Proline Building Block

One of the key fragments of Nirmatrelvir is the bicyclic [3.1.0] proline derivative **8** (Scheme 1), which is essential for the synthesis of the key western fragment intermediate **13** (Scheme 1). Several strategies have been attempted to provide this moiety with high yields, and the identification of an efficacious synthetic strategy for the bicyclic proline moiety has been essential for the development of a scalable pathway that ultimately led to the commercial process of the industrial synthesis of the drug. Multiple strategies have been reported during the years for the synthesis of this moiety, but, after evaluating all the possible approaches to afford the bicyclic [3.1.0] proline building block, researchers at Pfizer focused on the cyclopropanation of olefine **17** (Scheme 2) [19].

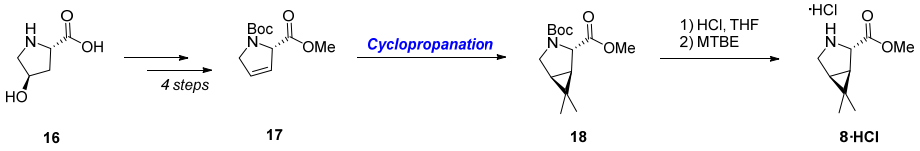

Scheme 2. Synthetic approach planned to afford the bicyclic [3.1.0] proline building block (**8**); THF = Tetrahydrofuran; MTBE = Methyl tert-butyl ether.

This strategy starts from commercially available compound **16**, which is inexpensive and already contains the correct stereocenter required for **8**. Compound **16** is converted into its derivative (**17**) following a strategy that was already reported on a multigram scale. The key step in the synthesis of the bicyclic [3.1.0] proline building block is the cyclopropanation of **17** (Scheme 3). Pfizer's researchers envisioned that this reaction could proceed with good enantioselectivity due to the steric hindrance provided by the gem-dimethyl group. Methods for the gem-dialkyl cyclopropanation of inactivated or weakly activated olefins reported in the literature were not very effective, until 2018, when Werth and Uyeda reported the cobalt-catalyzed dimethylcyclopropanation of olefins, where they employed a cobalt precatalyst in a complex with pyridine diimine (PDI) ligand L1 ($L1CoBr_2$),

2,2-dichloropropane as a carbene equivalent and zinc as a reductant [22]. Pfizer thus decided to focus on the development and optimization of a scalable process for the synthesis of **8** using Co-catalyzed dimethylcyclopropanation as the key reaction. Primarily, it is important to note that L1 was used as aligand in the initial campaign to adhere to the stringent project timeline. However, alternative ligands could be explored for further process optimization. Co-catalyzed cyclopropanation required the use of a zinc halide, as zinc salts seem to accelerate the reduction of the cobalt catalyst L1$CoBr_2$ to the active species L1CoBr. Following screening, zinc bromide was initially employed, but it faced reproducibility issues and handling difficulties owing to the hygroscopic nature of the salt. To encounter the need of an operationally friendly activation procedure and facile workup, the zinc halide was generated in situ, in order to eliminate the problems related to the direct handling of the salts. A comparison of zinc bromide, zinc iodide, and iodine revealed that the rate of cyclopropanation was higher in the presence of the iodide counteranion, but iodine resulted in a higher conversion than zinc iodide. Based on this observation, Pfizer's researchers moved forward with iodine as an activator for commercial production.

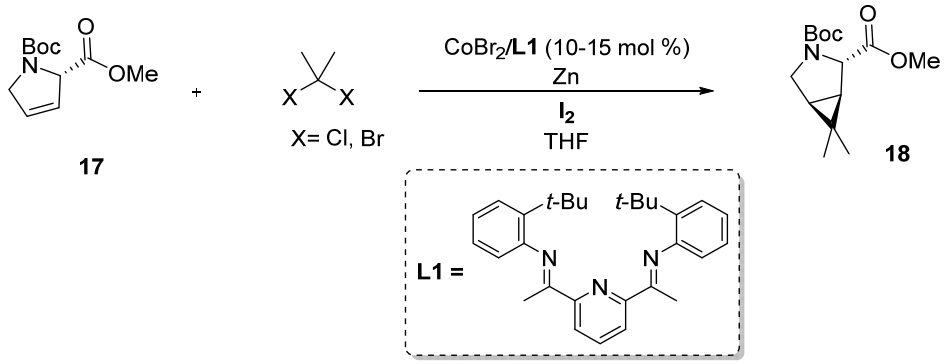

Scheme 3. Cobalt-catalyzed cyclopropanation of **17**; THF = Tetrahydrofuran.

While scaling up the process from a 100 g scale to kilograms, a reduction in conversion rates from 95% to 60–70% was observed. Suspecting catalyst instability as the cause of the conversion drop, they concentrated their efforts on gaining a deeper understanding of the process. Their investigations revealed that catalyst degradation started immediately after the introduction of the 2,2-dihalopropane starting material into the reactor. They also observed that, during the kilogram-scale reactions, zinc was not uniformly suspended in the reactor. The instability of the catalyst was therefore attributed to the rate of regeneration of the reduced form of the catalyst, which was lower than the rate of oxidative addition of 2,2-dihalopropane. This problem was due to a low stirring rate. In fact, after increasing the agitation rate in the reactor, they observed a huge increase in the conversion. Even if 2,2-dichloropropane was initially used by Pfizer as the starting material, its difficult obtainment in big quantities led to the decision to move forward with 2,2-dibromopropane as the starting material for the kilogram-scale process. One of the challenges that they had to face with the use of this reactant was the more rapid degradation of the catalyst, with respect to that observed with 2,2-dichloropropane. The problem was solved by reducing the rate of addition of 2,2-dibromopropane in the reactor, in order to allow the Co catalyst to convert to its reduced form and to avoid the accumulation of 2,2-dibromopropane in the reactor. After optimizing the cyclopropanation step of the synthesis, they focused on the deprotection of **18** and formation of **8**. The main problem was the purification of the product, which was addressed by crystallizing **8** and performing the final deprotection and isolation directly from the crude mixture after an acidic workup (Scheme 4).

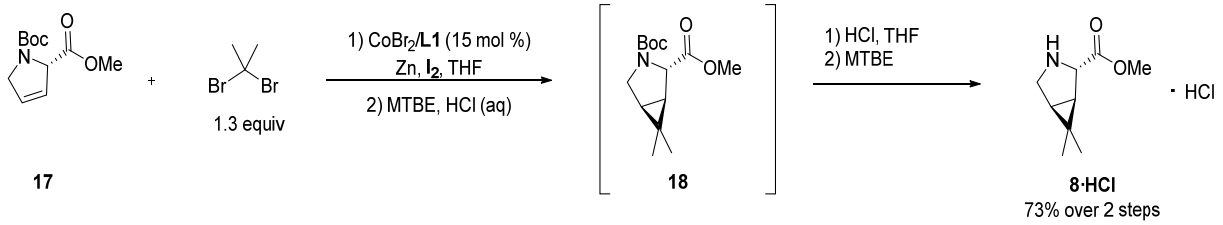

Scheme 4. Optimized scalable synthesis of **8** via Co-catalyzed cyclopropanation; THF = Tetrahydrofuran; MTBE = Methyl tert-butyl ether.

Compound **18** was then treated with HCl in THF leading to the removal of the Boc group and finally to the crystallization of **8·HCl** at a high purity, with a 50–60% isolated yield over two steps (i.e., cyclopropanation and deprotection). The addition of Methyl tert-butyl ether (MTBE) allowed us to improve the solubility of **8·HCl**, increasing the yield to >70%. The overall process was then executed on a 310 kg scale to produce **8·HCl** with a 73% yield over two steps.

3.2.2. Synthesis of the Western Fragment

As already mentioned in the previous paragraph, a key intermediate in the synthesis of Nirmatrelvir is the western fragment **13**, whose synthesis has been described by Algera et al. [19]. The discovery of a synthetic route for **13** led to the production of Nirmatrelvir in 4 steps in the first ever kilogram-scale manufacture of the drug shown in Scheme 5, which was further developed into the commercial route.

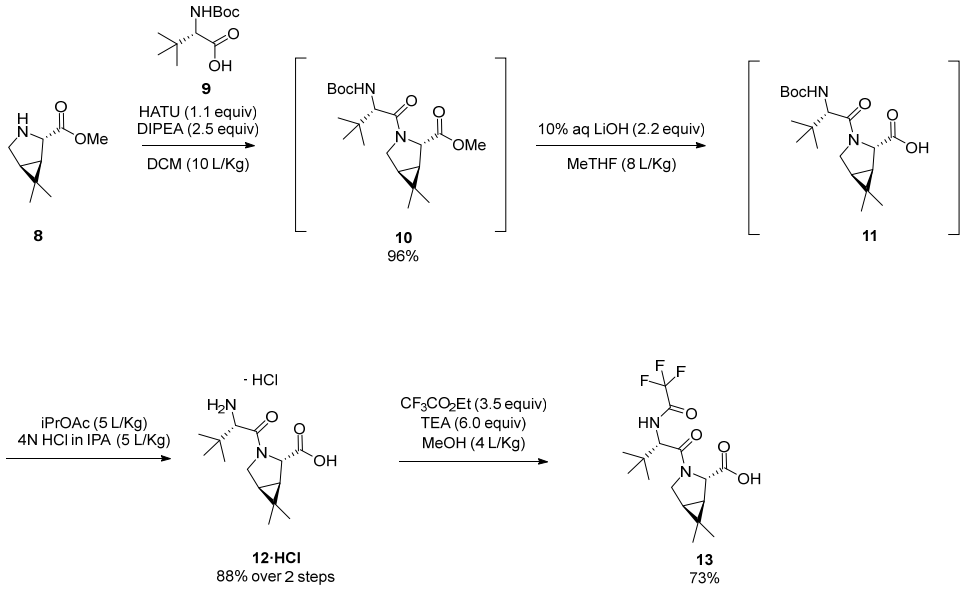

Scheme 5. First kilogram-scale synthesis of the western fragment HATU = Hexafluorophosphate Azabenzotriazole Tetramethyl Uronium, DIPEA = N,N-Diisopropylethylamine, DCM = Dichloromethane, THF = Tetrahydrofuran, iPrOAc = Isopropyl acetate, IPA = Isopropyl alcohol, TEA = Triethylamine, and MeOH = Methanol.

The western fragment 13 was eventually obtained from 19 and 20 through a convergent approach consisting of an amidation step.

Compound **19** (Scheme 6) is obtained through hydrolysis from the bicyclic [3.1.0] proline derivative **8·HCl**, bearing a methyl ester moiety. The high solubility of both **19** and its salts in aqueous conditions made the isolation of **19** challenging, so hydrolysis was

performed differently by dissolving **8·HCl** in a THF and water mixture, followed by treatment with LiOH causing the precipitation of the lithium carboxylate **19·Li** (Scheme 6).

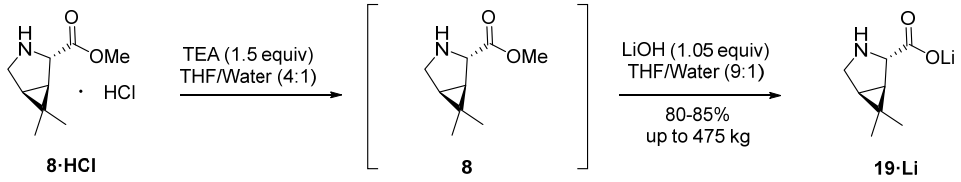

Scheme 6. Synthesis of 19-Li; TEA = Triethylamine; THF = Tetrahydrofuran.

19·Li was used for the screening of the amidation reaction with **20**, obtained from the reaction of commercially available L-tert-leucine with ethyl trifluoroacetate and sodium methoxide in methanol (Scheme 7). Following an aqueous work up, compound **20** was further purified by recrystallization from heptane (Scheme 7).

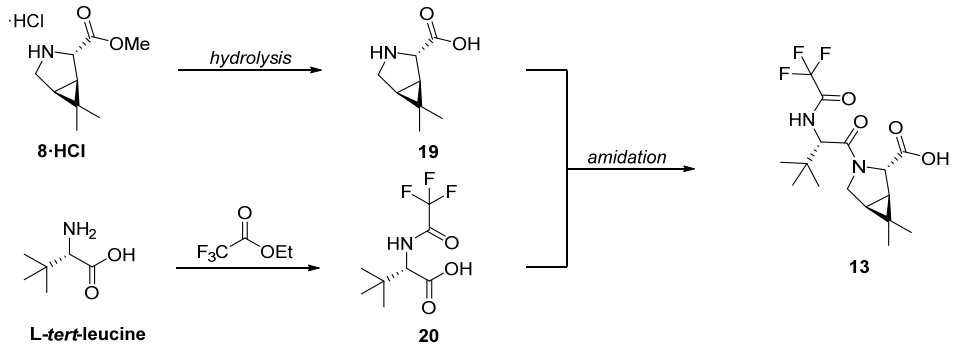

Scheme 7. Proposed convergent synthesis of **13**.

An initial screening of amidation conditions showed that the treatment of **20** with 1-Ethyl-3-(3-dimethylaminopropyl)carbodiimide (EDCI) and N-hydroxy succinimide produced a succinimidyl ester, which could react with **19·Li** to produce **13** with good yields and high stereochemical purity. So, after high-throughput screening to optimize the process and a laboratory scale-up, it was found that the use of 4-Toluenesulfonyl chloride (TsCl) in combination with 4-Dimethylaminopyridine (DMAP) in THF as the solvent afforded **13** in a high yield with minimal impurities (Scheme 8). These conditions also presented advantages like the availability and cost of TsCl and the ease of using THF in industrial plants. DCM was not further evaluated due to its low environmental compatibility.

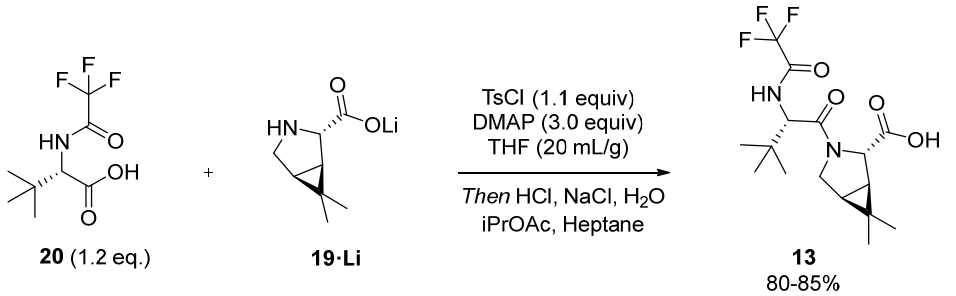

Scheme 8. Initial manufacture of **13**; TsCl = 4-Toluenesulfonyl chloride, DMAP = 4-Dimethylaminopyridine, THF = Tetrahydrofuran, and iPrOAc = Isopropyl acetate.

The reaction was performed by dissolving **20** in THF. TsCl and DMAP were then added to activate **20**, before the introduction of **19·Li** to avoid the tosylation of **19**. The reaction was then quenched with HCl and brine to facilitate the aqueous workup. The isolation of the reaction product directly from THF was difficult, but it could be crystallized in iPrOAc with the addition of heptane as an antisolvent. Further process development adjustments were made on both the amidation reaction and the hydrolysis of methyl ester **8**. In particular, while the lithium salt of **19** was simple to obtain, it was not suitable for a scale-up. In fact, **19·Li** was found to be rich in LiCl impurities and hygroscopic. For these reasons, different alternatives were screened. In the end, the best solution appeared to be the sodium salt that was chosen for ongoing development, thanks to its more favorable physical characteristics compared to the lithium salt and because it could be easily obtained replacing LiOH with NaOH in the hydrolysis of **8**. The conditions tested for the preliminary attempts of the amidation process with **19·Na** were the same identified for the reaction with **19·Li**. However, despite the effectiveness of the process, expensive and undesirable reagents, like DMAP, and the solvent exchange from THF to isopropyl alcohol (IPA) were required. In addition, the preferable use of liquid reagents led to the replacement of TsCl with Methanesulfonyl chloride (MsCl), which led to a complete conversion without the use of DMAP, but using only Triethylamine (TEA). Scheme 9 shows the optimized conditions used for the conversion of **19·Na** to **13.**

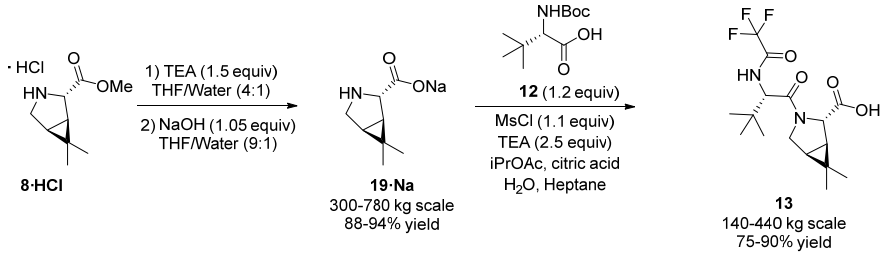

Scheme 9. Optimized preparation of western fragment **13**; TEA = Triethylamine, THF = Tetrahydrofuran, MsCl = Methanesulfonyl chloride, and iPrOAc = Isopropyl acetate.

3.2.3. Synthesis of the Eastern Fragment

Another key building block of Nirmatrelvir is represented by the primary amide **14·HCl**, also referred to as the eastern fragment, obtained via the aminolysis of **24·TsOH** [20]. The first-generation synthesis of **14·HCl** (Scheme 10) provides **24·TsOH** starting from the diastereoselective alkylation of the lithium dianion of Boc-dimethyl glutarate **21**. The alkylation using bromoacetonitrile resulted in the predominant formation of a single diastereomer of nitrile **22**. The nitrile group was then subjected to reduction, leading to the formation of lactam **23**. Subsequent treatment with p-toluenesulfonic acid facilitated deprotection, yielding **24·TsOH** as a crystalline intermediate, thus obviating the necessity for column chromatography purification. Subsequently, **24·TsOH** was subjected to Boc-protection to yield **23**, which was isolated and reacted with ammonia, resulting in the formation of the aminolysis product **25**. Treatment of this intermediate with hydrochloric acid in IPA allowed the deprotection of the amine, yielding **14·HCl**.

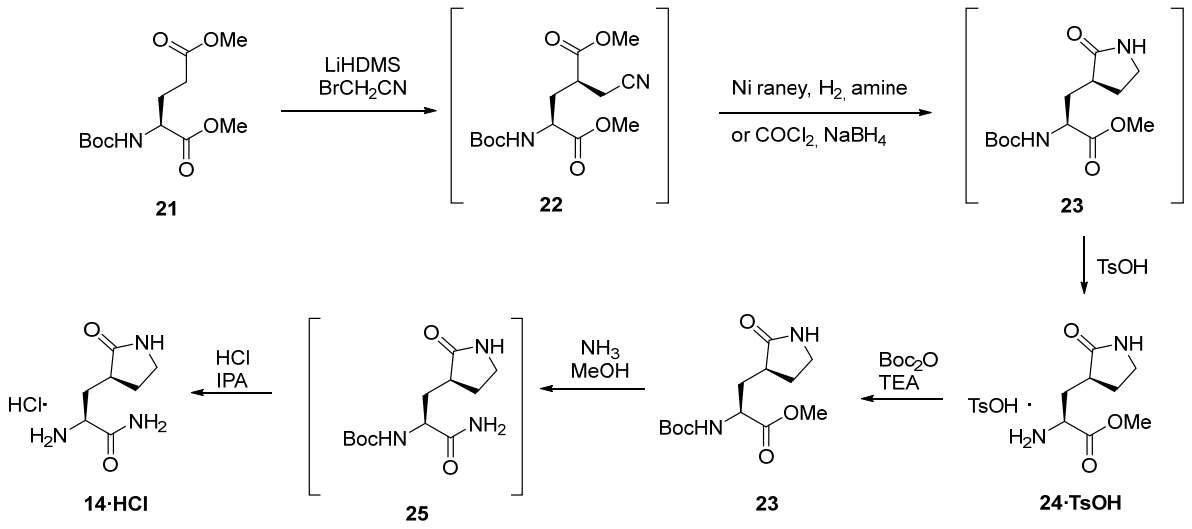

Scheme 10. First-generation synthesis of 14·HCl; LiHDMS = Lithium bis (trimethylsilyl)amide, TEA = Triethylamine, MeOH = Methanol, and IPA = Isopropyl alcohol.

Even if this synthetic strategy was suitable for the large-scale production of **14·HCl**, researchers at Pfizer recognized the opportunity to streamline the process. In particular, the main problems with the first-generation route were: (i) the need for protection and deprotection steps to reduce the formation of side products; (ii) the formation of **23** twice in the synthesis, with the need of isolating the intermediate the second time it appeared, resulting in additional processing time and waste; and (iii) the fact that **24·TsOH** was not suitable for direct aminolysis due to the sluggishness of the reaction with ammonia and the production of different impurities (Scheme 11). Moreover, the obtained **14·HCl** still contained residual traces of isopropyl alcohol, contributing to some of the remaining mass balance. The use and storage of **14·HCl** also presented safety risks due to the breaking of its agglomerates, which led to the release of flammable solvents. For all these reasons, researchers started to look for an alternative synthetic strategy to afford **14·HCl**.

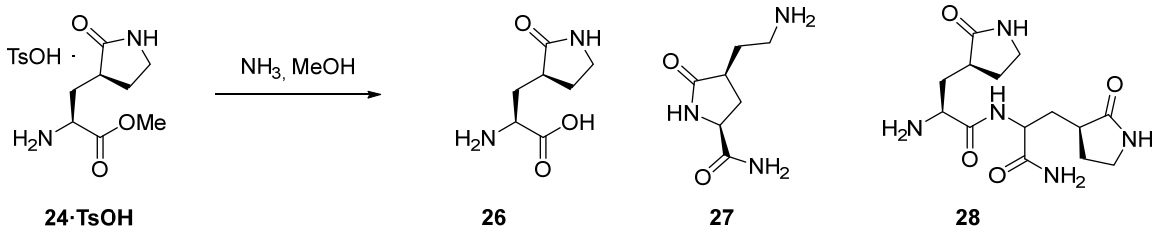

Scheme 11. Impurities obtained from the aminolysis of 24·TsOH; MeOH = Methanol.

Given that the supply chain for **24·TsOH** had already been established at Pfizer, the optimization of the route began with the exploration of conditions enabling the direct aminolysis of **24·TsOH**. The objective was to achieve high yields, minimize impurity formation, and reduce reaction times. It was envisioned that the use of a Lewis acid during the reaction could accelerate aminolysis reaction times, increasing the reactivity of the ester toward substitution and preventing the formation of pyroglutamate **27** and dimer **28** (Scheme 11). An evaluation of various Lewis acids was ultimately performed, leading to the implementation of $MgSO_4$ as the preferred reagent for this reaction, as it is an insoluble salt easily removable via the filtration of the reaction mixture. The reaction performed in the presence of $MgSO_4$ resulted in high yields and minimal formation of the hydrolysis by-product **26**.

The next challenging task involved devising a method for isolating **14·HCl** after Boc-deprotection. Analysis of the reaction mixture indicated the presence of the correct product, together with magnesium ions and tosylate as impurities that required removal. The decision to isolate HCl salt instead of tosylate salt was due to the difficulties faced during the attempt to obtain **14·TsOH** as a crystalline solid. With this purpose, DMF was found to be an efficient solvent to purge undesired by-products, including magnesium chloride and p-toluenesulfonic acid, while facilitating the high recovery of **14·HCl**. Moreover, to shift the equilibrium from **14·TsOH** toward **14·HCl**, an excess of HCl was used in the reaction. Furthermore, HCl in IPA could be used without the risk of a high level of residual Mg $(OTs)_2$, which is poorly soluble in this solvent. So, after aminolysis, filtration through Celite was employed to remove insoluble materials and methanol was exchanged with DMF to solubilize the side products. HCl in IPA was added to prompt the crystallization of **14·HCl**, and finally dichloromethane was introduced as an antisolvent to enhance product recovery (Scheme 12, path A). Although this process offered notable advantages, it also presented several challenges that needed to be addressed. Initially, **14·HCl** isolated through this method contained organic impurities and residual DMF, which posed difficulties in effective removal, due to the stability concerns of **14·HCl** at elevated temperatures required for solvent evaporation. Furthermore, the use of DCM as an antisolvent was undesirable for environmental reasons. An investigation for alternative solvent systems was pursued, eventually leading to the use of methanol and water as the process medium—methanol was found to be a potential candidate because it was the same solvent used in the previous aminolysis reaction. Since **14·HCl** remained moderately soluble in methanol, an antisolvent was required to increase product recovery. Isopropyl alcohol has been evaluated as the best antisolvent to improve the recovery of solids. Crystallization using MeOH and water as the process solvents and IPA as the antisolvent resulted in the crystallization of **14·HCl** at high purity and with minimal residual solvent (Scheme 12, path B).

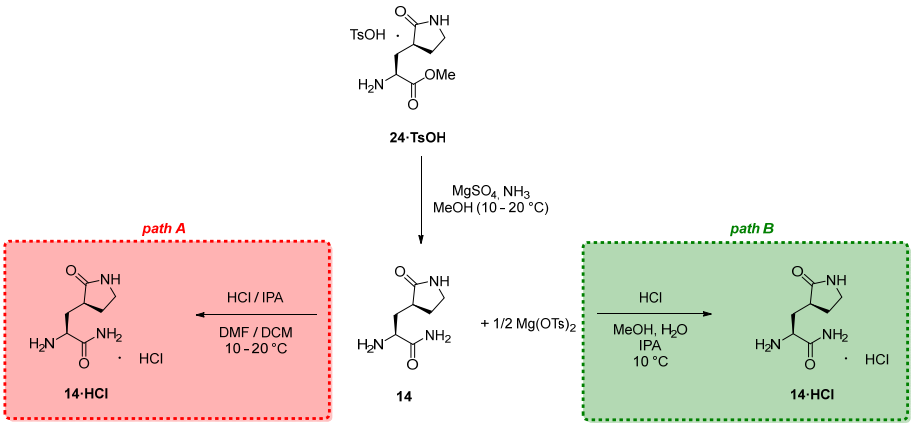

Scheme 12. Final synthetic route from **24·TsOH** to **14·HCl**; ·TsOH = p-Toluensolfonic acid salt, ·HCl = Hydrochloride salt DMF = N,N-Dimethylformamide, DCM = Dichloromethane, and IPA = Isopropyl alcohol.

Further optimizations after the scale-up of the process led to reducing hold times after HCl addition in IPA and a lower temperature (10 °C) for the isolation of **14·HCl**. These modifications were implemented because the stability of **14·HCl** appeared to be dependent on the hold time and temperature.

3.3. Application of Flow Chemistry in Nirmatrelvir Synthesis

The industrial approach used by Pfizer for Nirmatrelvir's synthesis involved expensive and challenging chemicals or required extended reaction times, which heightened the

risk of side-product formation due to epimerization. Flow chemistry offers a promising approach for the synthesis of bioactive compounds, like Nirmatrelvir, due to its numerous advantages over traditional batch synthesis methods [23]. Veeramani's group figured that the formation of the amide bond between the western fragment and lactam **29**, which already embodies the -CN moiety, would be more efficient; therefore, they directed their efforts toward synthesizing fragment **29** (Scheme 13).

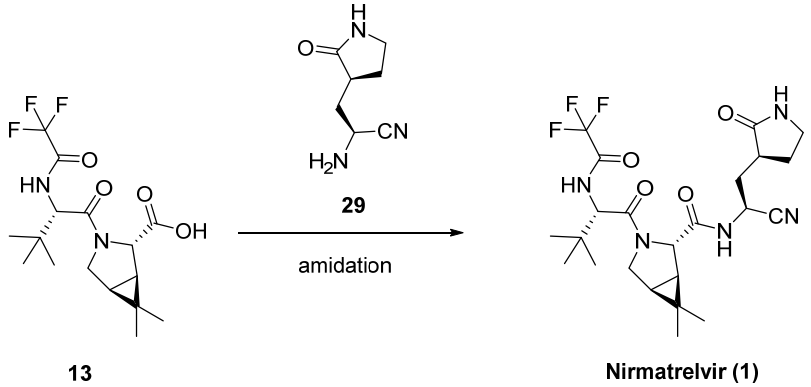

Scheme 13. Direct synthesis of Nirmatrelvir (**1**) via the amidation of **13** with nitrile **29**.

The main difficulty of this pathway was the obtainment of **29** at sufficient purity to respect the quality requirements defined for advanced intermediates taken forward to the final API.

The optimized synthesis of **29** is depicted in Scheme 14 and starts with the conversion of commercially available ester **23** to carboxamide **25** using a concentrated solution of ammonia in methanol. This solution was prepared by passing ammonia gas through a precooled solution of **23** in methanol**.** Dehydration of **25** was initially attempted with trifluoroacetic anhydride (TFAA), but the formation of heavy suspension in the reaction mixture led us to prefer the use of propanephosphonic acid anhydride (T3P), which allows the obtainment of the nitrile-bearing fragment **29.** The Boc deprotection step was challenging because of the formation of the impurity **14·HCl**, obtained from the hydrolysis of the cyano group to an amide. Several reagents and reaction conditions were attempted with the aim of minimizing the hydrolysis of **29·HCl** to **14·HCl** and obtaining **29** in a good and persistent yield. The best conditions resulted in the use of aqueous HCl in THF. Purification of **29** included the simple precipitation of hydrochloride salt (**29·HCl**) from the reaction mixture with > 95% purity, even if 1–2% of the amino-amide **14·HCl** persisted as an impurity.

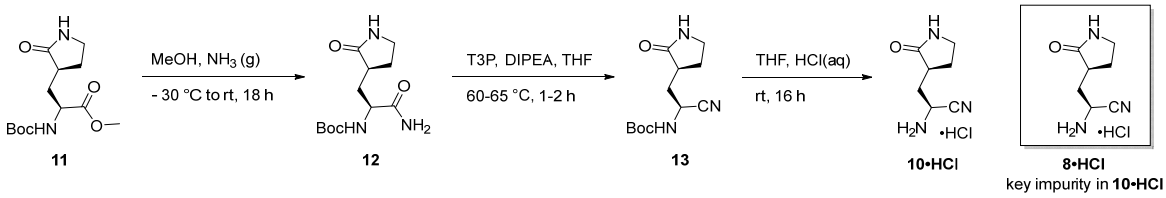

Scheme 14. Synthesis of **29·HCl** from **23;** MeOH = Methanol, rt = room temperature, DIPEA = N,N-Diisopropylethylamine, THF = Tetrahydrofuran, and ·HCl = Hydrochloride salt.

Having obtained **29** with sufficient purity, T3P was used to carry out the amidation of **13** with **29** to produce **1**. The main advantage of using T3P for amide bond formation is that the small quantity of impurity **14** was not detrimental to the final yield. In fact, the amidation of **13** with **14** produced impurity 15, which then underwent dehydration by the

same T3P present in the reaction mixture to produce the desired final product. Nirmatrelvir (**1**) was obtained with a ~97% yield overall (Scheme 15)

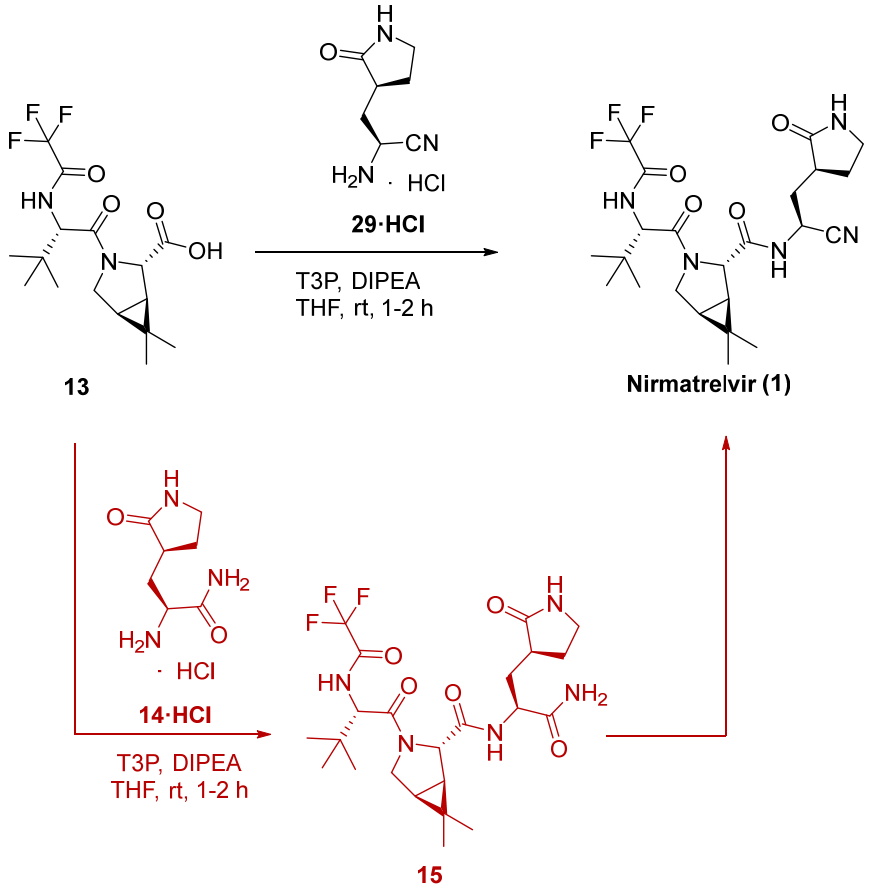

Scheme 15. Amidation of **13** with **29·HCl** using T3P in presence of the impurity **14·HCl**; ·HCl = Hydrochloride salt, T3P = Propanephosphonic acid anhydride, DIPEA = N,N-Diisopropylethylamine, THF = tetrahydrofuran, and rt = room temperature.

The main advantage of this procedure is that it avoids the use of the Burgess reagent in favor of T3P, which presents low toxicity, long shelf-life stability, and easy handling. Veeramani's group further improved the synthetic process, performing the final dehydration of impurity **15** to **1** using continuous flow chemistry. The main advantage of flow reactors, in comparison to batch reactors, is their more favorable surface-to-volume ratio, which enhances heat and mass transfer to obtain desired products with higher yields and better selectivity. Flow chemistry also allows us to easily perform sensitive reactions, to have better control of exothermic reactions, and to easily scale-up the process for large-scale production.

Specifically, the enhancement of the dehydration stage involved preventing the liquid stream from evaporating. This allowed us to use higher temperatures beyond the boiling points of the solvents, consequently reducing reaction durations. Figure 5 shows the schematic representation of the flow experimental setup that was employed.

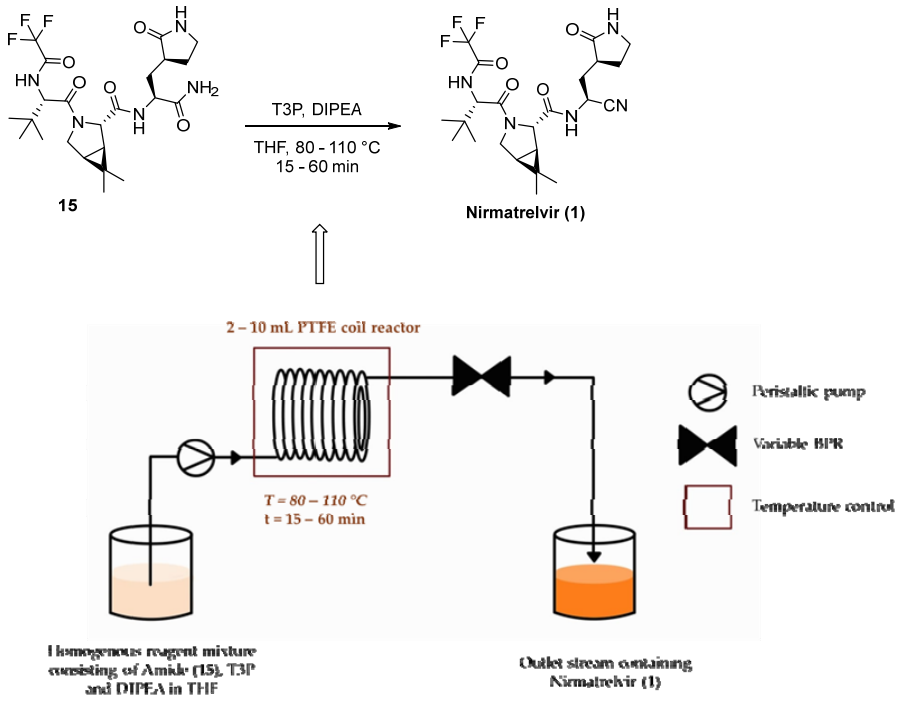

Figure 5. Schematic representation of the continuous-flow setup used for synthesis of **1** via the T3P-mediated dehydration of amide **15**; T3P = Propanephosphonic acid anhydride, DIPEA = N,N-Diisopropylethylamine, THF = Tetrahydrofuran, PTFE = Polytetrafluoroethylene, and BPR = Back Pressure Regulator.

A complete conversion of carboxamide **15** to Nirmatrelvir **1** was obtained when the reaction was performed at 100 °C for a residence time of 30 min, using 2.5 equiv of N,N-Diisopropylethylamine (DIPEA) and 2.0 equivalents of T3P. The yield and purity obtained are comparable to those obtained by the conventional batch process.

It is possible to conclude that the continuous-flow process can create advantages for the synthesis of Nirmatrelvir, as it allows us to reduce the reaction times from the 12–16 h necessary for the batch process to just 30 min. Moreover, the flow process allows us to avoid the use of high temperatures and extreme pressures. Currently, more studies are being performed to obtain Nirmatrelvir from the reactions of **13** and **14** through a T3P-mediated tandem amidation dehydration in flow.

3.4. Multicomponent Approach

An alternative way to improve the synthetic process to obtain Nirmatrelvir is the use of multicomponent reactions. This class of reactions is being increasingly appreciated in medicinal chemistry, because it enables us to synthesize biologically active molecules in a more sustainable, cost-effective, and rapid way.

Preschel et al. proposed the synthesis of Nirmatrelvir based on the multicomponent assembly of N-trifluoroacetyl-tert-leucine **33**, chiral bicyclic imine **31**, and isocyanide **32** through a diastereoselective Ugi-type three-component reaction (U-3CR) (Scheme 16) [24].

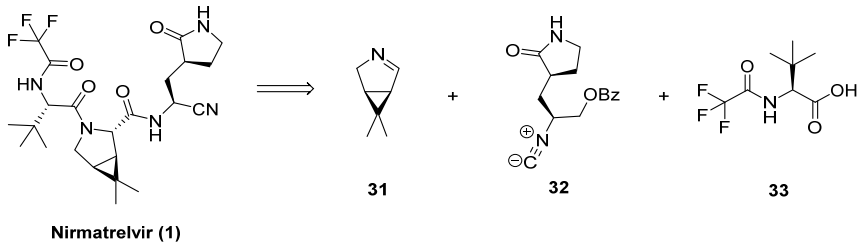

Scheme 16. Retrosynthesis of Nirmatrelvir using a multicomponent approach.

Chiral imine **31** was prepared by the monoamine oxidase N (MAO-N) biocatalyzed oxidation of amine **34**. This reaction proceeded with an enantiomeric excess higher than 99% (Scheme 17). Biocatalysis has become a relevant tool in the pharmaceutical industry, because it can provide a more sustainable and efficient method to produce APIs and pharmaceutical intermediates. Enzymes are in fact renewable and biodegradable materials, they can react in aqueous conditions and they have high chemo- and enantioselectivity, therefore avoiding protection or deprotection steps.

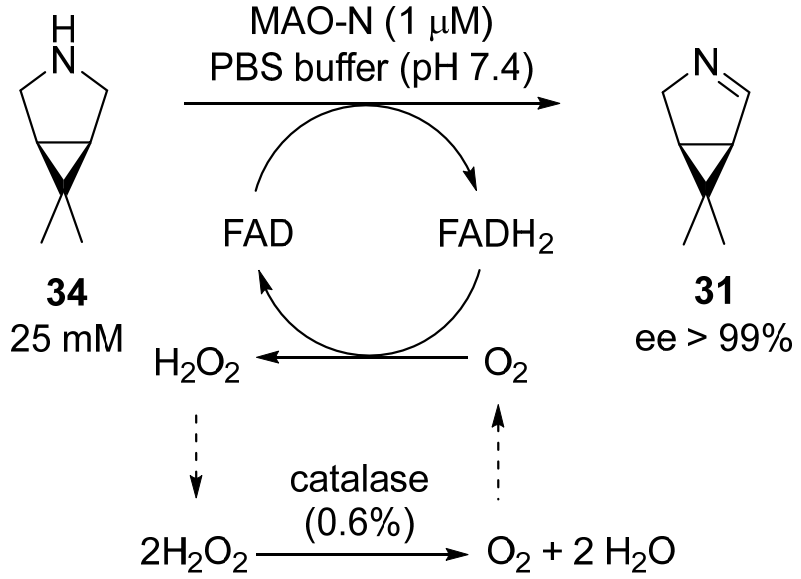

Scheme 17. Biocatalytic synthesis of **31** using MAO-N**;** MAO-N = Monoamine oxidase, PBS = Phosphate-buffered saline, FAD = Flavin Adenine Dinucleotide, and ee = enantiomeric excess.

The isocyanide moiety was obtained from the Boc-protected amino ester **23** (Scheme 18), which is commercially available. Compound **23** was converted into primary alcohol **35** using $LiBH_4$. Compound **35** was then protected as a benzoate ester to produce **36**. Boc-cleavage, followed by the formylation of the resulting amine, produced formamide **37,** which was then dehydrated with triphosgene (0.66 equiv) in the presence of TEA (10 equiv) in DCM at −78 °C to produce isocyanide **32** as an isolable, stable, crystalline solid (Scheme 18). The same results can alternatively be obtained by the treatment of **37** with TFAA (1.9 equiv), TEA (8 equiv), and THF at 0 °C for 30 min. The obtained crystals were analyzed through X-ray diffraction; thus, the structure and absolute configuration of compound **32** were confirmed.

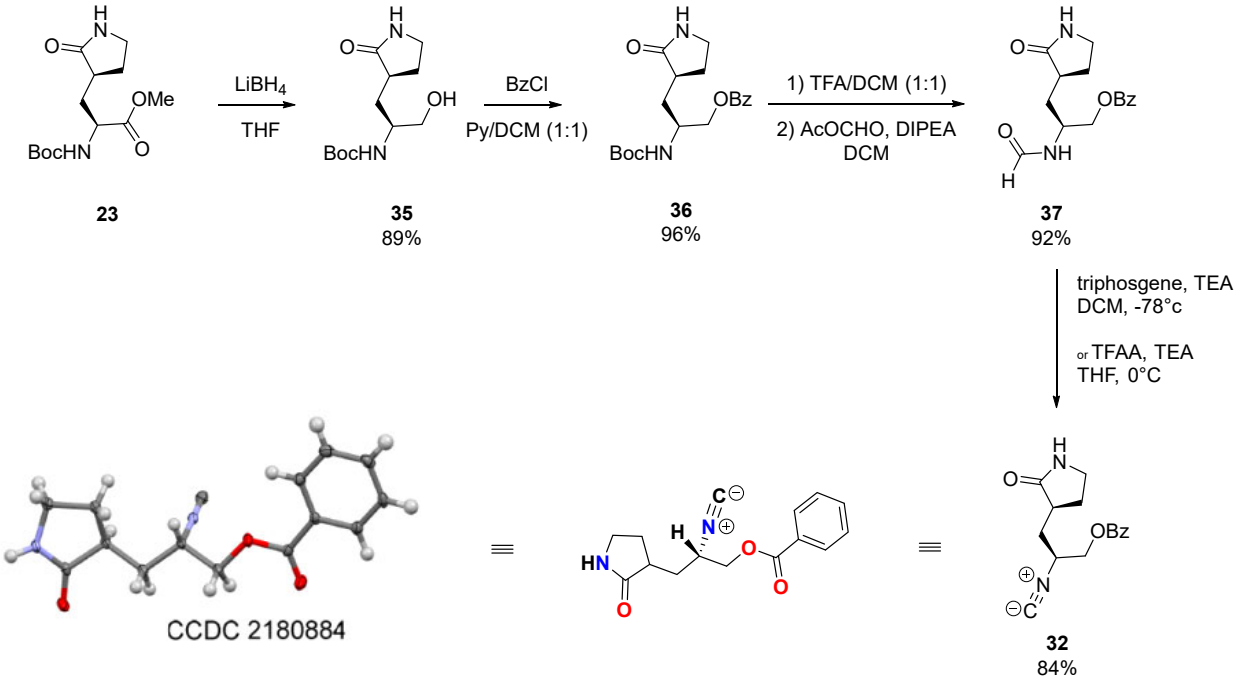

Scheme 18. Synthesis of isocyanide **32** and X-ray structure of **32**; THF = Tetrahydrofuran, BzCl = Benzoyl chloride, Py = Pyridine, DCM = Dichloromethane, TFA = Trifluoroacetic acid, AcOCHO = Acetic formic anhydride, DIPEA = N,N-Diisopropylethylamine, TEA = Triethylamine, and TFAA = Trifluoroacetic anhydride.

The three fragments were combined together in a U-3CR, as reported in Scheme 19. The enantioselectivity of the reaction is driven by imine **31**, because the gem dimethyl moiety shields the concave face of the bicyclic system. In a first attempt, isocyanide **32**, imine **31**, and carboxylic acid **33**, obtained from the trifluoroacetylation of L-tert-Leucine, were reacted in DCM to produce **38** as a 5:1 mixture of diastereomers. The low enantioselectivity was initially connected to incomplete stereo-induction at the newly formed stereocenter. After further examination, it was found that the procedure used to obtain **33** led to some erosion of its stereochemistry. A new attempt was therefore made using commercially available acid **33** (>98 e.e.), which reacted with imine **31** and isocyanide **32** to produce compound **38** in a 68% isolated yield and > 25:1 dr. Methanolysis of the benzoate ester produced primary alcohol **39**, which was then deprotected and oxidized with a one-pot procedure involving PhI $(OAc)_2$/TEMPO with amonium acetate as the nitrogen source, to produce Nirmatrelvir in an 83% yield (Scheme 19).

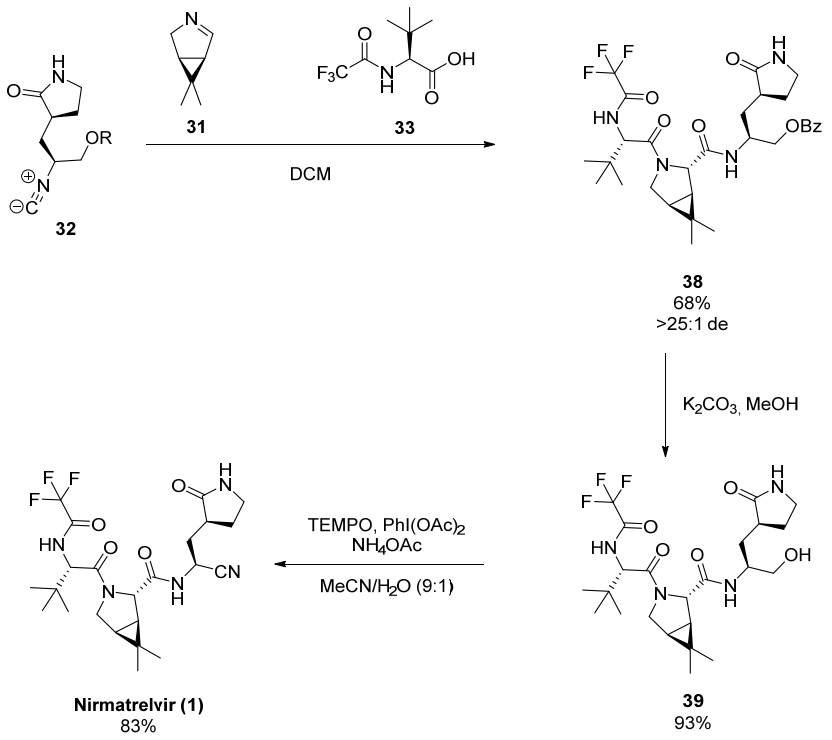

Scheme 19. Synthesis of Nirmatrelvir through U-3CR. DCM = dichloromethane, de = diastereomeric excess, TEMPO = 2,2,6,6-tetramethylpiperidin-1-yl)oxyl, and MeCN = acetonitrile.

It was observed that, by streamlining the synthetic pathway, compound **32** could be obtained without intermediate purifications and with minimal mass loss. The U-3CR reaction was performed in methanol, allowing a one-pot combination of the Ugi reaction and of the saponification step. The product was directly used for the final step to produce Nirmatrelvir in a 70% yield, which is higher than the one obtained over the three last steps with intermediate purifications (48%) (Scheme 20).

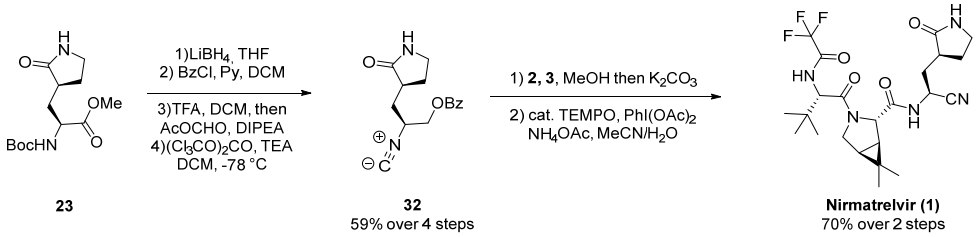

Scheme 20. Streamlined synthesis of Nirmatrelvir through U-3CR; THF = tetrahydrofuran, BzCl = Benzoyl chloride, Py = pyridine, DCM = dichloromethane, TFA = Trifluoroacetic acid, AcOCHO = Acetic formic anhydride, DIPEA = N,N-Diisopropylethylamine, TEA = triethylamine, MeOH = Methanol, TEMPO = 2,2,6,6-tetramethylpiperidin-1-yl)oxyl, and MeCN = acetonitrile.

3.5. Sustainable Synthesis

The immediate high demand of Nirmatrelvir during the COVID-19 pandemic led to environmental concerns connected to the industrial process, which makes large use of peptide coupling reagents and organic solvents. Since the beginning, it has been clear that there was a need to optimize the existing synthetic pathways to Nirmatrelvir to make them greener and cheaper, two characteristics that are also fundamental for the distribution of Paxlovid in the Global South. For these reasons, many efforts were put into the development of a new industrial process that could have a lower environmental impact

while being economically attractive. An interesting approach to the synthesis of Nirmatrelvir has been suggested by Kincaid et al., with a seven-step, three-pot route, reaching the targeted product in a 70% overall yield [25]. The key points of this sustainable approach are (i) the amide bond formation steps, obtained with green technologies that allow us to avoid the use of common coupling reagents (e.g., HATU, DCC, COMU, etc.), and (ii) the dehydration step of the primary amide into the corresponding nitrile without using the Burgess reagent and chlorinated solvents, which are employed in the parental Pfizer procedure. The entire process is reported in Scheme 21.

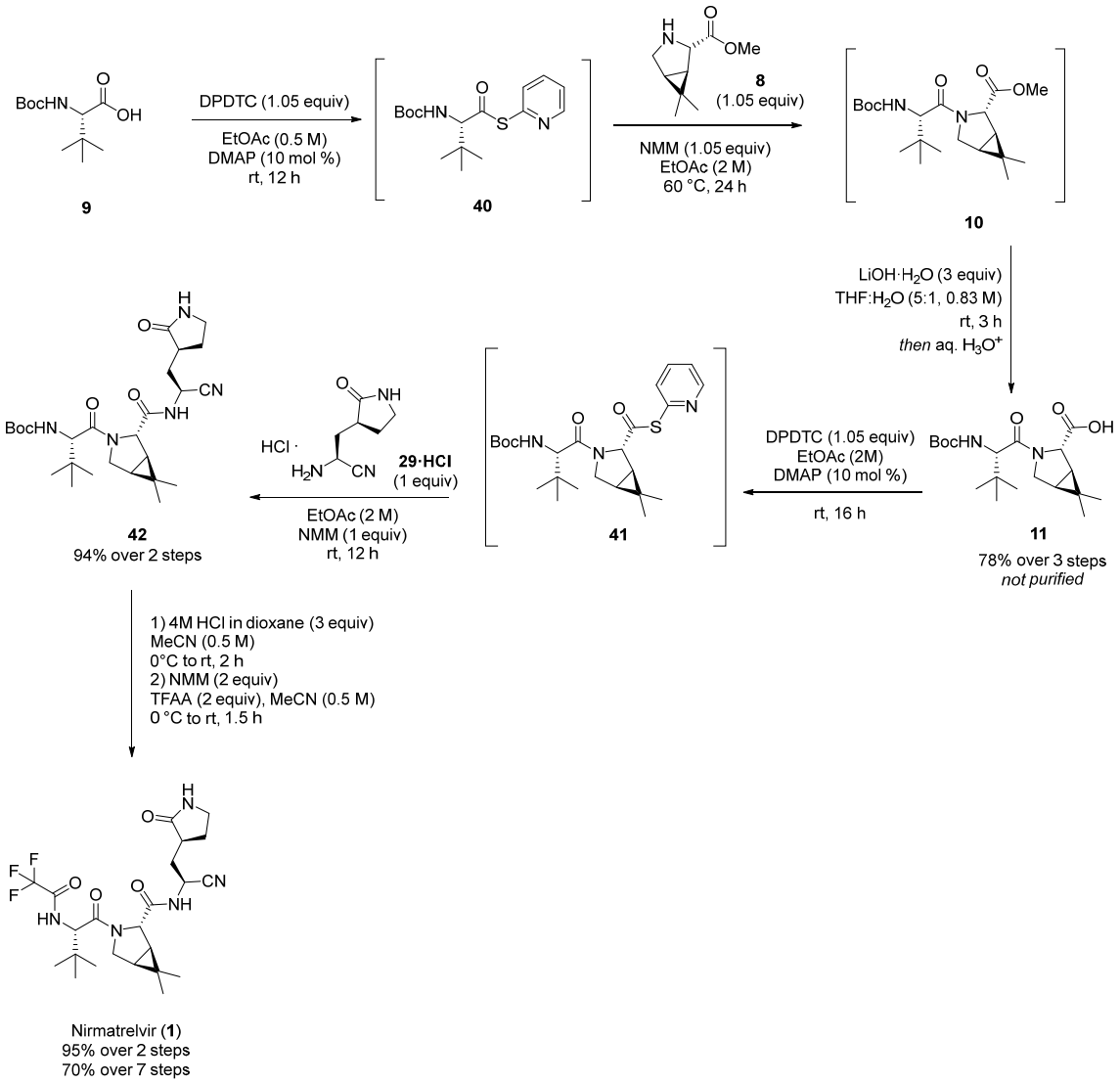

Scheme 21. Overall route to Nirmatrelvir featuring thioester intermediates **40** and **41** en route to peptides **10** and **42**, respectively. DPDTC = di-2-Pyridyldithiocarbonate, EtOAc = Ethyl acetate, DMAP = 4-(dimethylamino)pyridine, rt = room temperature, NMM = N-Methylmorpholine, THF = Tetrahydrofuran, MeCN = Acetonitrile, and TFAA = Trifluoroacetic anhydride.

The sequence features a one-pot thioesterification/amide bond formation using di-2-pyridyldithiocarbonate (DPDTC). This reagent activates carboxylic acids and, beyond avoiding the use of classical coupling reagents, it also prevents epimerization while allowing the easy removal of the 2-mercaptopyridine by-product with an aqueous alkaline solution. Furthermore, the produced 2-mercaptopyridine can be readily turned back into DPDTC, showcasing a crucial characteristic for a reagent employed in an environmentally

friendly process. Intermediate thioesters **40** and **41** are stable and potentially isolable, simplifying potential large-scale use and manufacture. However, in this route, isolation and purification were not required. After the formation of thioester **40**, in the presence of DMAP, the reaction mixture went through an in-flask treatment with **8** and N-Methylmorpholine (NMM) in EtOAc affording the desired amide intermediate **10**. Compound **10** was not isolated, but directly dissolved in aqueous THF in the presence of LiOH. After the reaction, the mixture was neutralized with aqueous HCl and extracted with EtOAc obtaining **11** with a 78% yield over three steps. The resulting intermediate **11** did not require purification, since the small amounts of impurities present, primarily 2,2′-dipyridyldisulfide, had no synthetic consequences. Carboxylic acid **11** was subjected to a second thioesterification under the same reaction conditions previously discussed. Finally, the eastern fragment was introduced by reacting **41** with **29·HCl** in EtOAc in the presence of NMM, affording **42** with a 94% yield over two steps. The subsequent N-Boc deprotection of **42** was performed using a concentrated solution of HCl/dioxane in MeCN. It seems that HCl is preferable to trifluoroacetic acid (TFA) as the latter leads to lower yields and is involved in the formation of multiple side products, including various materials resulting from epimerization. Solvent and an excess of HCl were removed in vacuo and the amine hydrocloride salt obtained was treated with trifluoroacetic anhydride (TFAA) and NMM to install the trifluoroacetamide moiety. TFAA and NMM were then removed via aqueous washes, affording Nirmatrelvir in a 95% yield over two steps with 95% purity confirmed by HPLC. A brief focus on the synthesis of reagent **29** is summarized in Scheme 22. Compound **29** was obtained from **23**, a readily accessible methyl ester, which underwent conversion into the corresponding primary amide **25** utilizing a documented procedure [13]. At this stage, the primary amide underwent a dehydration step employing a more environmentally friendly approach compared to Pfizer's use of the Burgess reagent with a chlorinated solvent. In fact, the nitrile-bearing intermediate has been obtained by applying technology based on "amide exchange" [26,27]. This technology uses commercially available fluoroacetonitrile as the sacrificial acceptor of water under palladium-catalyzed conditions. The treatment of **25** in these conditions produced **30**, with a 93% yield. Crystallization of **30** was needed to eliminate impurities and by-products coming from the use of fluoroacetonitrile. Subsequent N-Boc deprotection was achieved using HCl in the presence of a sacrificial nitrile, such as MeCN, to reduce undesired competitive hydrolysis and, at the same time, performing the azeotropic removal of residual water in **30** using recoverable toluene under a high vacuum. These two precautions minimized the formation of undesired by-products **29a** and **29b** affording **29** as HCl salt with a 95% yield and only 3% hydrolysis product.

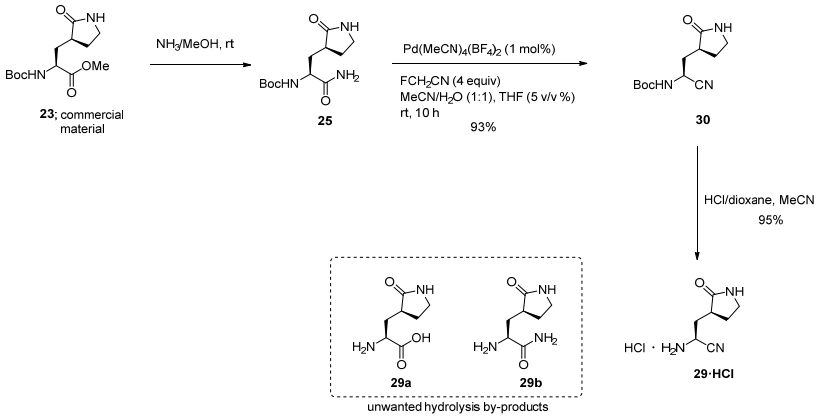

Scheme 22. Preparation of aminonitrile **29·HCl** from readily available starting material **23**; MeOH = Methanol, rt = room temperature, MeCN = Acetonitrile, THF = Tetrahydrofuran, and ·HCl = Hydrochloride salt.

This convergent route to Nirmatrelvir has been accomplished in a 70% overall yield, a considerable improvement on the 48% reported by Pfizer for the first-generation process. After achieving these interesting results, the process to obtain Nirmatrelvir was further streamlined. The initial seven-step strategy could in fact be reduced by two steps by eliminating the necessity of removing the protecting group from the starting N-Boc-L-tert-leucine (Scheme 23) [28]. To achieve this, the trifluoroacetamide derivative of L-tert-leucine (**20**) was used as the starting material. This approach allowed us to perform with the same reagent both the deprotection step and the subsequent insertion of the trifluoroacetamide fragment. The main issue encountered when using the trifluoroacetamide derivative of L-tert-leucine **20** as starting material was the challenging generation of the corresponding thioester. This thioester was essential for the reaction with the sodium salt of bicyclic proline **10·Na** to yield intermediate **13**. Following the low yields obtained using the corresponding HCl salt of **20**, attributed to the compound's instability, several amide coupling reagents were screened. This resulted in the adoption of propanephosphonic acid anhydride (T3P) as the coupling reagent. T3P was chosen due to its efficiency, practicality in usage and workup, absence of stereochemical issues regarding diastereomer formation, environmental considerations, and economic accessibility. Therefore, carboxylic acid **20** was activated by T3P in the presence of DIPEA at −10 °C over a 1 h period. Bicyclic proline sodium salt **10·Na** was then added portionwise at 0 °C, followed by dilution with anhydrous EtOAc. The resulting mixture was then warmed slowly to rt with continuous stirring for 20 h. Aqueous acid was added to remove side products generated from T3P. After removing the aqueous medium and concentrating the ethyl acetate, **13** was obtained in high yields (from 93% to 96% using a concentration of 0.5 M in EtOAc). After obtaining **13**, this intermediate had to be reacted with **29·HCl** to afford Nirmatrelvir (**1**). T3P was also evaluated for this amide bond formation: **29·HCl** carries a primary amine with high reactivity, so the mixing of all reagents in a single reaction flask in the presence of DIPEA (T < 0 °C) with vigorous stirring led to complete starting-material conversion within three hours, as evidenced by TLC analysis. After this time, the reaction was diluted with EtOAc and subjected to an aqueous wash using 1 M HCl. Solvent removal in vacuo produced crude **1**, which was then exposed to EtOAc/MTBE (1:10). Subsequent solvent removal provided solvated Nirmatrelvir MTBE.

In conclusion, this optimization campaign of the previous seven-step, three-pot route that produced Nirmatrelvir with a 70% overall yield resulted in a streamline of the process and the development of a three-step, one-pot sequence that allowed us to create Nirmatrelvir as MTBE solvated with an overall 64% yield.

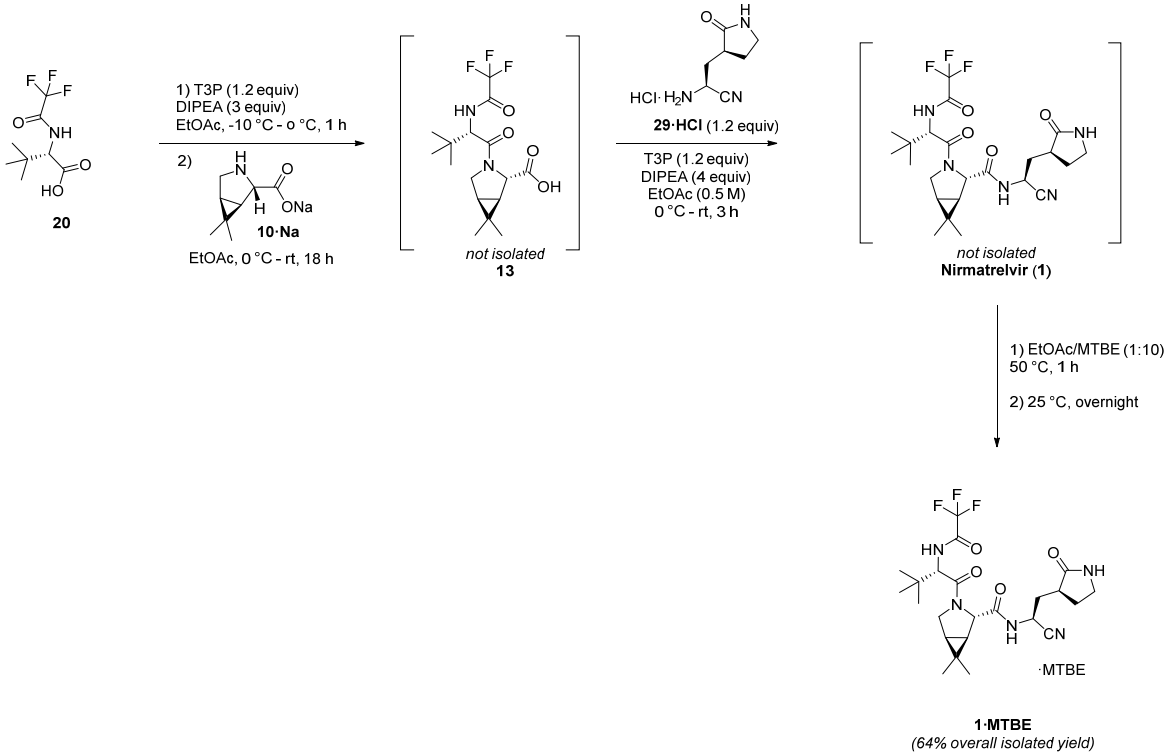

Scheme 23. The 1-pot, 3-step synthesis of Nirmatrelvir MTBE solvate (**1**). T3P = Propanephosphonic acid anhydride, DIPEA = N,N-Diisopropylethylamine, EtOAc = Ethyl acetate, rt = room temperature, MTBE = Methyl tert-butyl ether, and ·MTBE = Methyl tert-buthyl ether solvate.

4. Industrial Scale-Up of Nirmatrelvir Synthesis

Pfizer's proposed synthesis of Nirmatrelvir offers several opportunities for optimization toward industrial-scale production. Key areas for improvement include addressing cost-intensive components, such as starting materials **8**, **9**, and **13**; the coupling reagent HATU; the Burgess reagent used for amide dehydration; and enhancing the yield of trifluoroacetylation to obtain compound **13**. Additionally, the initial step required purification via column chromatography.

Appasaheb et al. made a screening of several coupling reagents and reaction conditions to improve the yield of the coupling reaction between the bicyclic proline and N-Boc-L-tert-leucine, without using the expensive HATU as the coupling reagent [29]. The most favorable outcomes were observed when employing a combination of N,N′-Dicyclohexylcarbodiimide (DCC) and Hexafluorophosphate Benzotriazole Tetramethyl Uronium (HBTU); however, the use of HBTU was ruled out due to safety concerns. Employing 2.1 equivalents of DCC, 0.5 equivalents of 1-Hydroxy-7-azabenzotriazole (HOAt), and 3 equivalents of NMM in DCM compound **10** was obtained with a 88% yield. Proline **8**, identified as a primary cost contributor, is deliberately utilized as the limiting reagent in this process, with the reaction proceeding for 24 h at room temperature. The use of DMF as a co-solvent allowed us to increase the yield only from 88% to 90%, so the improvement was not considered significant and therefore not necessary.

To avoid column chromatography, intermediate **10** on the crude mixture was used directly for the successive saponification step. After an aqueous workup, intermediate **11** was precipitated from a solution of acetonitrile by the addition of water. The best results on this telescoped procedure allowed us to obtain **11** with a 75% yield over two steps and with 73% purity confirmed by HPLC (Scheme 24).

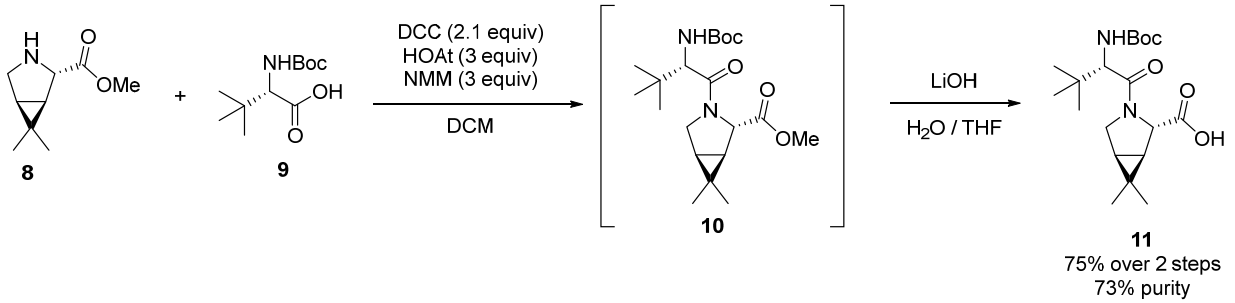

Scheme 24. Telescoped procedure to provide **11** without column chromatography; DCC = Dicyclohexyl carbodiimide, HOAt = 1-Hydroxy-7-azabenzotriazole, NMM = N-Methylmorpholine, DCM = Dichloromethane, and THF = Tetrahydrofuran.

After the deprotection of the amine, the yield of the trifluoroacetylation step was improved up to 98% using TFAA in MeOH, instead of trifluoro ethyl acetate, with an excess of DIPEA (Scheme 25).

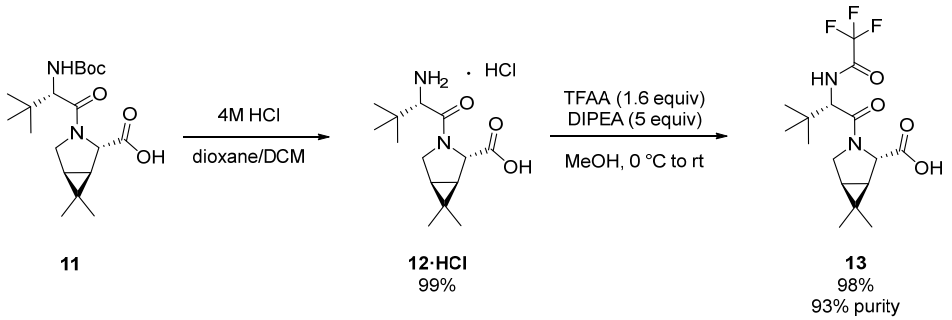

Scheme 25. Optimized trifluoroacetylation step; DCM = Dichloromethane, TFAA = Trifluoroacetic anhydride, DIPEA = N,N-Diisopropylethylamine, MeOH = Methanol, and rt = room temperature.

The dehydration of the amide functional group using the Burgess reagent presented several challenges concerning cost, availability and reagent stability during storage, as well as the removal of by-products. Additionally, the removal of dichloromethane (DCM) in the amidation reaction was recommended for environmental consideration. After the screening of different conditions, Appasaheb et al. found TFAA and T3P to be similarly effective. Increasing the quantity of T3P, some impurities formed in the reaction mixture, but they were removed through crystallization from MTBE/EtOAc. TFAA was found to provide better results and allowed us to obtain Nirmatrelvir (**1**) in a 90% overall yield. A screening of the reaction conditions was made and the best results were obtained using NMM as a base. Crystallization led to an MTBE solvated product with a 85% yield. MTBE-free crystals were obtained through crystallization in heptane/iPrOAc with the same conditions reported in the Pfizer procedure (Scheme 26).

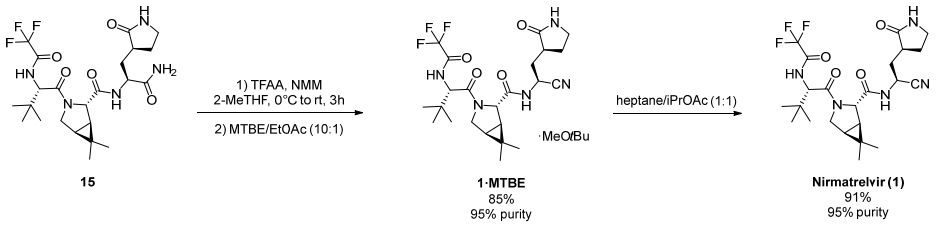

Scheme 26. Optimized procedure for the dehydration of amide functionality; TFAA = Trifluoroacetic anhydride, NMM = N-Methyl morpholine, 2-MeTHF = 2-Methyl tetrahydrofuran, rt = room

temperature, MTBE = Methyl tert-buthyl ether, EtOAc = Ethyl acetate, ·MTBE = Methyl tert-buthyl ether solvate, and iPrOAc = Isopropyl acetate.

Due to the ability of TFAA to both dehydrate the amide and produce the trifluoroacetylated product, a one-pot process was attempted. The first attempt to obtain Nirmatrelvir's MTBE solvated product in a telescoped manner led to the obtainment of Nirmatrelvir with a 63% yield (Scheme 27).

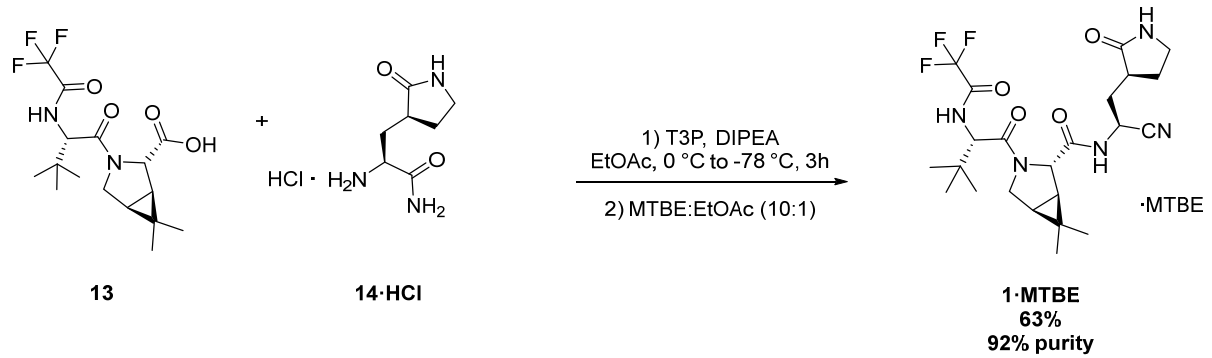

Scheme 27. Telescoped amidation dehydration by Appasaheb et al.; ·HCl = Hydrochloride salt, T3P = Propanephosphonic acid anhydride, DIPEA = N,N-Diisopropylethylamine, MTBE = Methyl tert-buthyl ether, EtOAc = Ethyl acetate, and ·MTBE = Methyl tert-butyl solvate.

The possibility to perform the final amidation dehydration step through a telescoped process was studied in more detail by Algera et al., starting from the new screening of different reaction conditions for both the amidation and dehydration steps [30].

The coupling reaction involving **13** and **14** was optimized using EDCI with HOPO in methyl ethyl ketone (MEK) and T3P with N-methylimidazole (NMI) in MeCN, which yielded the most favorable outcomes and were thus subjected to further investigation. These reaction conditions exhibited compatibility with various solvents and bases. T3P facilitated a high conversion rate and, as previously mentioned, it was also effective in the dehydration process. However, notable quantities of impurities **43** and **44** were generated under these conditions (Figure 6). Additionally, the use of MeCN as the solvent posed challenges for the subsequent aqueous workup step.

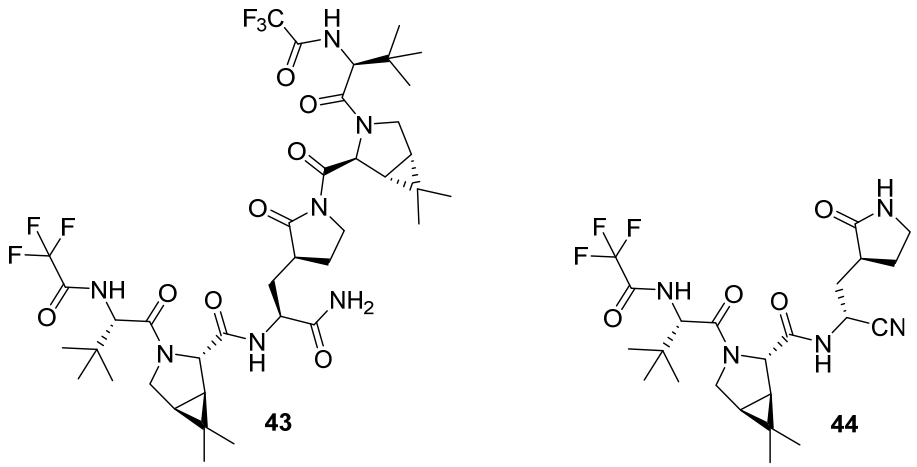

Figure 6. Main impurities from the T3P process; T3P = Propanephosphonic acid anhydride.

This led to the selection of EDCI and HOPO in MEK as the best conditions for the amidation step.

For the amide dehydration step, Burgess-type reagents (Figure 7) were excluded for atom economy reasons, as three equivalents of reagent were needed.

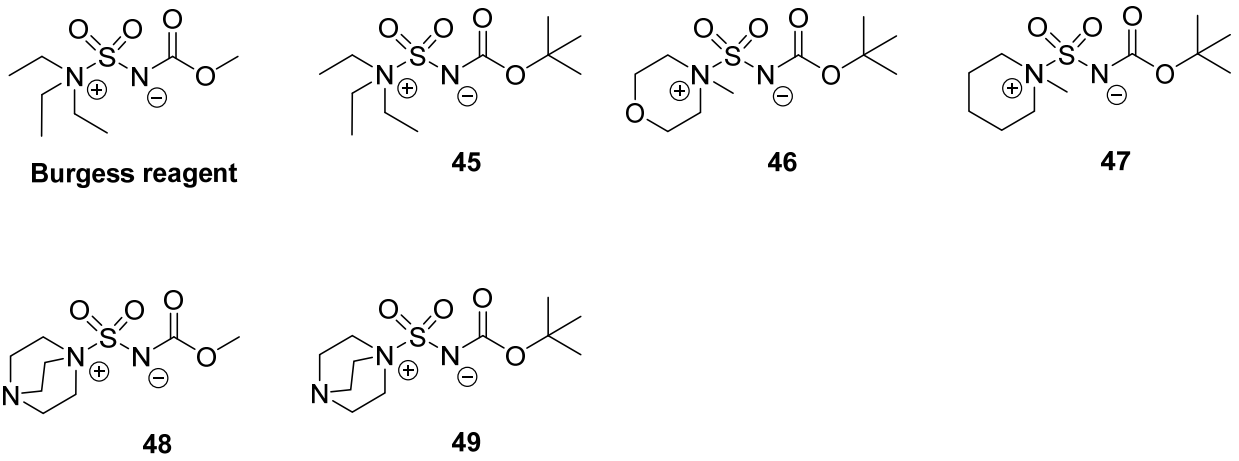

Figure 7. Burgess reagent alternatives explored.

After the screening of different dehydration conditions, T3P and NMI in MeCN and TFAA and NMM in iPrOAc were found as the most promising. T3P caused the formation of impurity **44** reported in Figure 6, and was found to be more inclined toward the epimerization of the nitrile stereocenter; so, TFAA was selected for use in the dehydration step.

The telescoping of the amidation and dehydration steps was favored by the elimination of MTBE. This also allowed us to increase the reproducibility. The solvents for the two steps were then evaluated, considering the need for an aqueous workup between the amidation and the dehydration steps and the preferability to use a single solvent in the two steps. MEK allowed us to control moisture in the dehydration step, important for the sensibility of TFAA to water, but the dehydration step was slow, creating concerns regarding TFAA accumulation. iPrOAc favored the dehydration step, but moisture control was more difficult. Moreover, **14** is poorly soluble in iPrOAc. Considering all these aspects, iPrOAc was finally chosen as the preferred solvent.

The main impurities formed during the telescoped sequence were acylureas **50** and **51** (Figure 8), caused by EDCI-promoted amidation, but their formation could be prevented by increasing the amount of HOPO used in the reaction (0.75 equiv). Basic conditions could lead to the rearrangement impurity **52** and subsequently **53**. After the dehydration step, a small quantity of starting material **15** was still present. The epimerization that caused the formation of **44** could be avoided by controlling the pH and temperature. TFA adducts **54** and **55** formed during the dehydration step were accurately controlled defining plant parameters (Figure 8).

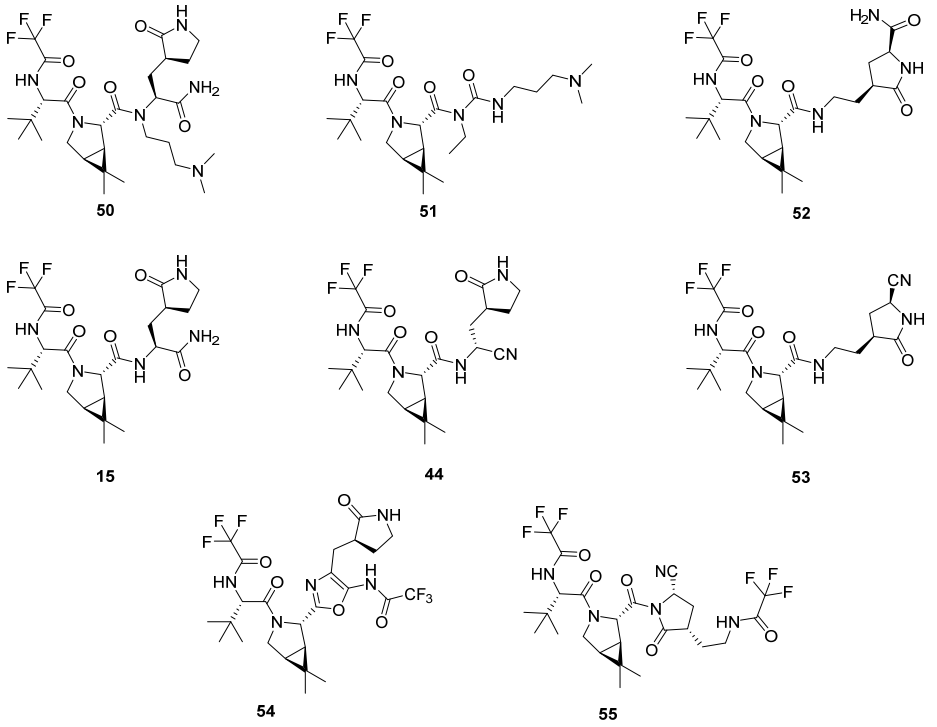

Figure 8. Process-related impurities in the Nirmatrelvir commercial process.

The optimized procedure reported in Scheme 28 was first tested at the laboratory scale with 5 g (60% yield), then 100 g (65% yield), and finally 53 kg in the manufacturing plant (75% yield, 95 kg of **1**). The increase in the yield with bigger quantities is due to the better control of moisture.

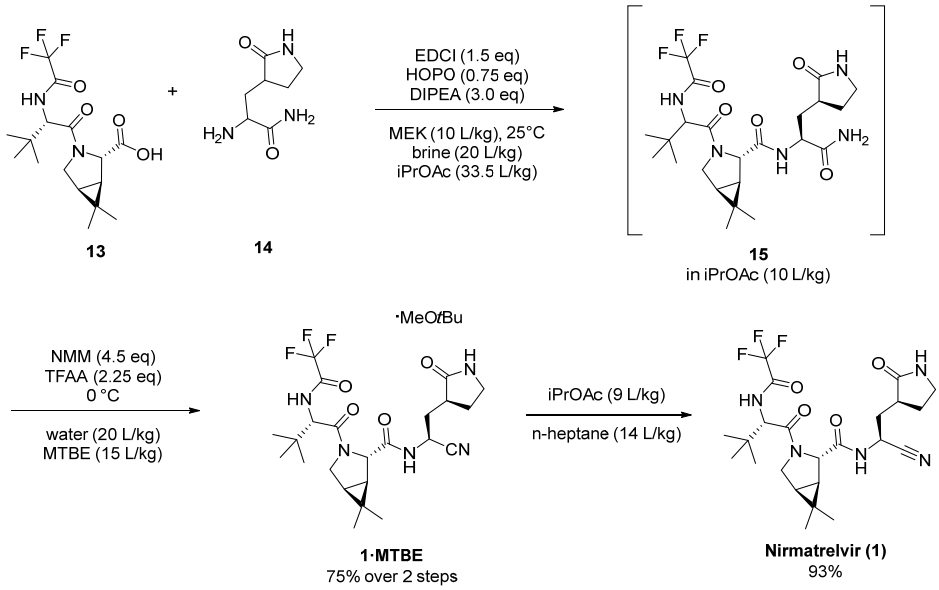

Scheme 28. Enabled telescoped amidation dehydration sequence; EDCI = *N*-(3-dimetilaminopropil)-*N*′-etilcarbodiimide, HOPO = Hydroxypyridine-N-oxide, DIPEA = *N*,*N*-Diisopropylethylamine, MEK = Methyl ethyl ketone, iPrOAc = Isopropyl acetate, NMM = *N*-Methylmorpholine, TFAA = Trifluoroacetic anhydride, MTBE = Methyl tert-buthyl ether, and ·MTBE = Methyl tert-buthyl solvate.

5. Variants and Modifications to Nirmatrelvir

Even after the conclusion of the COVID-19 pandemic, a strong demand persists for new therapeutics targeting SARS-CoV-2, due to the development of drug resistance (ACS central science, 2023, 9.8: 1658–1669) [31]. Moreover, numerous global drug discovery initiatives have been undertaken to develop treatments for post-infection scenarios and to pre-emptively address potential future pandemics. The literature extensively documents endeavors aimed at enhancing the potency of Nirmatrelvir through structural modifications or synthesizing compounds with improved properties compared to existing patented and commercial drugs. To this purpose, notable findings in this regard have been reported, and we decided to include three examples of chemical modifications of Nirmatrelvir, made in order to improve potency and reduce drug resistance.

One of the proposed modifications is the electrophilic warhead. In 2024, Elshan et al. described the discovery of **CMX990** (**57**, Figure 9), a potent SARS-CoV-2 M^{pro} inhibitor bearing a novel trifluoromethoxymethyl ketone warhead [32]. The authors explored SAR across all regions of this peptidomimetic in order to reach the final product, now going through Phase 1 clinical trials. This compound showed an excellent balance of physicochemical and ADME (absorption, digestion, metabolism, and excretion) properties, allowing for high potency in target engagement as well as favorable PK properties. Compond **57** was validated in a biochemical assay for SARS-CoV-2 M^{pro}, where it was demonstrated that the compound acts as a reversible inhibitor (IC_{50} = 23.4 nM). Compond **57** also exhibited the inhibition of replications of eight SARS-CoV-2 variants, including alpha, delta, and omicron.

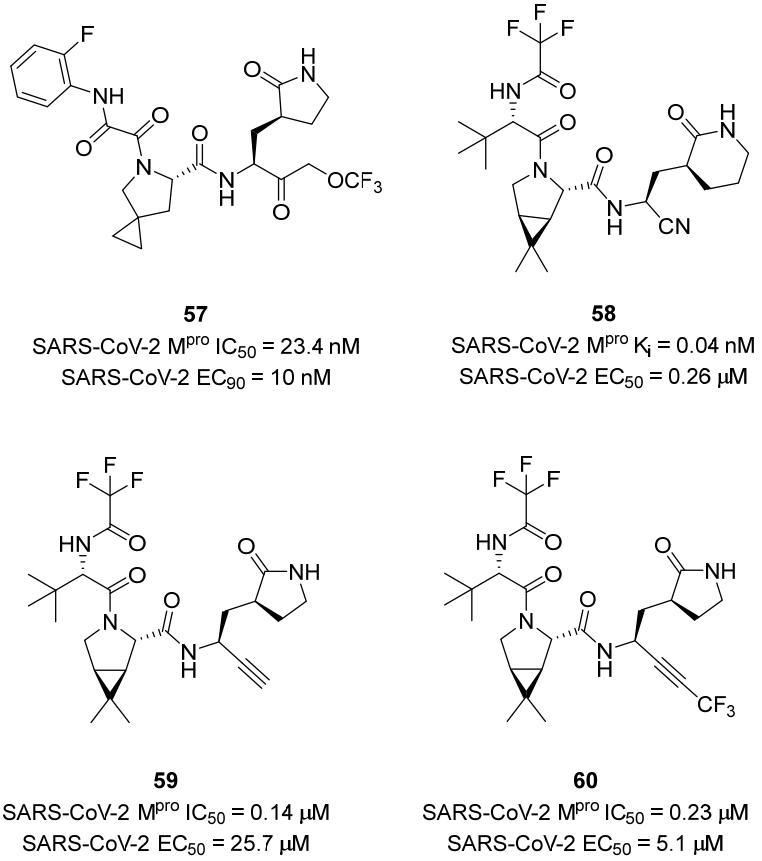

Figure 9. Main structural modifications of Nirmatrelvir.

In a recent study, Ghosh et al. focused on modifying P1 and P4 of Nirmatrelvir to enhance inhibitory activity [33]. Their goal was to improve binding within the S1 subsite

and fill the hydrophobic pocket in the S4 subsite of the M^{pro}. Various alkyl, aryl, halogenated acetamide, carbamate, and urea derivatives were evaluated as P4 ligands, combined with five-membered and six-membered lactams as P1 ligands. The findings show that P4 amide derivatives are significantly more potent in comparison to carbamate and urea ones. Notably, several inhibitors with a six-membered lactam ring and halogenated P4 amides showed a marked increase in inhibitory and antiviral activities compared to Nirmatrelvir. Specifically, compound **58** (Figure 9), featuring a P1 six-membered lactam and P4 trifluoro acetamide groups, demonstrated a three-fold improvement in antiviral activity in VeroE6 cells and retained efficacy against variants such as delta and omicron, comparable to remdesivir. High-resolution X-ray crystallography of 5e-bound SARS-CoV-2 M^{pro} revealed that the six-membered lactam ring forms stronger hydrogen bonds and fills the hydrophobic pocket more effectively than the five-membered lactam ring in Nirmatrelvir. These results highlight the potency-enhancing effects of the P1 six-membered lactam, providing valuable insights into the optimization of Nirmatrelvir derivatives and related compounds for M^{pro} inhibition.

Another interesting modification to Nirmatrelvir's P4 residue was made in 2023 by Brewitz et al., who decided to replace the nitrile warhead with an alkyne group [34]. Nirmatrelvir-derived alkyne **59** (Figure 9) was found to inhibit M^{pro} ~5-fold less efficiently than Nirmatrelvir (**1**) with an IC_{50} ~0.14 μM, but its inhibition of SARS-CoV-2 progression in cells is ~11-fold less efficient than Nirmatrlevir (EC50 ~25.7 μM) (Figure 9). Compound **59** was also tested through MTT cells' viability assay and was found to be non-cytotoxic, even if further studies should be performed on the metabolism of alkynes in animals. The alkyne warhead was also functionalized with aryl groups that could fit into the S' pocket, but all the synthetized derivatives showed a ~50-fold to ~80-fold decreased inhibition of M^{pro} compared to that of **59**. The functionalization of the alkyne with a $–CF_3$ group instead presented interesting results: compound **60** (Figure 9) showed, in fact, a similar potency to **59** with an IC_{50} ~0.22 μM, but the inhibition of the progression of SARS-CoV-2 in infected VeroE6 cells was ~5-fold more efficient than that of **59** (EC_{50} ~5.1 μM) and only ~2-fold less efficient than Nirmatrelvir (**1**) (EC_{50} ~2.2 μM). Even if both **59** and **60** are less efficient than Nirmatrelvir, this study shows that appropriately functionalized alkynes have potential for the inhibition of SARS-CoV-2 M^{pro} and SARS-CoV-2 progression in cells.

6. Conclusions

The global urgency to counteract the COVID-19 pandemic has provided significant advancements in antiviral research, leading to the discovery of Nirmatrelvir as a potent inhibitor of SARS-CoV-2 M^{pro}. Combined with ritonavir and marketed as Paxlovid™, this compound represents the first oral treatment for COVID-19. This review has described various synthetic approaches for the synthesis of Nirmatrelvir from Pfizer's original strategy to innovative and more sustainable approaches, such as flow chemistry and multicomponent reactions. Moreover, several examples of Nirmatrelvir modifications, produced to overcome drug resistance, have been discussed. Looking forward, the synthesis and optimization strategies outlined in this review not only enhance the production efficiency of Nirmatrelvir, but also pave the way for future therapeutic interventions. By adopting more sustainable and scalable synthetic methods, the industry can better respond to current and future pandemics. Additionally, the innovative strategies discussed here can serve as a foundation for developing new antiviral agents with improved efficacy and safety profiles. Continued research and developments in this area hold promise for expanding known antiviral therapies.

Author Contributions: Conceptualization, A.C. and D.P.; methodology, M.G. and F.M.; software, D.P.; validation, A.C. and V.F.; formal analysis, A.C. and D.P.; investigation, M.G. and F.M.; resources, A.S..; data curation, A.C., A.S., V.F. and D.P.; writing—original draft preparation, M.G. and F.M.; writing—review and editing, A.C., A.S., V.F. and D.P.; visualization, A.C. and D.P.;

supervision, A.C. and D.P.; project administration, A.C. and D.P.; funding acquisition, A.S. All authors have read and agreed to the published version of the manuscript.

Funding: This research was supported by EU funding within the NextGeneration EU-MUR PNRR Extended Partnership initiative on Emerging Infectious Diseases (Project no. PE00000007, INF-ACT).

Conflicts of Interest: The authors declare no conflicts of interest.

References

1. De Vries, M.; Mohamed, A.S.; Prescott, R.A.; Valero-Jimenez, A.M.; Desvignes, L.; O'Connor, R.; Steppan, C.; Devlin, J.C.; Ivanova, E.; Herrera, A.; et al. A comparative analysis of SARS-CoV-2 antivirals characterizes 3CL(pro) inhibitor PF-00835231 as a potential new treatment for COVID-19. *J. Virol.* **2021**, *95*, e01819-20. https://doi.org/10.1128/jvi.01819-20.
2. Lamb, Y.N. Nirmatrelvir Plus Ritonavir: First Approval. *Drugs* **2022**, *82*, 585–591. https://doi.org/10.1007/s40265-022-01692-5.
3. Citarella, A.; Dimasi, A.; Moi, D.; Passarella, D.; Scala, A.; Piperno, A.; Micale, N. Recent Advances in SARS-CoV-2 Main Protease Inhibitors: From Nirmatrelvir to Future Perspectives. *Biomolecules* **2023**, *13*, 1339. https://doi.org/10.3390/biom13091339.
4. Bege, M.; Borbás, A. The Design, Synthesis and Mechanism of Action of Paxlovid, a Protease Inhibitor Drug Combination for the Treatment of COVID-19. *Pharmaceutics* **2024**, *16*, 217. https://doi.org/10.3390/pharmaceutics16020217.
5. Karniadakis, I.; Mazonakis, N.; Tsioutis, C.; Papadakis, M.; Markaki, I.; Spernovasilis, N. Oral Molnupiravir and Nirmatrelvir/Ritonavir for the Treatment of COVID-19: A Literature Review with a Focus on Real-World Evidence. *Infect. Dis. Rep.* **2023**, *15*, 662–678. https://doi.org/10.3390/idr15060061.
6. Akinosoglou, K.; Schinas, G.; Gogos, C. Oral Antiviral Treatment for COVID-19: A Comprehensive Review on Nirmatrelvir/Ritonavir. *Viruses* **2022**, *14*, 2540. https://doi.org/10.3390/v14112540.
7. Marzi, M.; Vakil, M.K.; Bahmanyar, M.; Zarenezhad, E. Paxlovid: Mechanism of Action, Synthesis, and In Silico Study. *BioMed Res. Int.* **2022**, *2022*, 7341493. https://doi.org/10.1155/2022/7341493.
8. Shen, J.X.; Du, W.W.; Xia, Y.L.; Zhang, Z.B.; Yu, Z.F.; Fu, Y.X.; Liu, S.Q. Identification of and Mechanistic Insights into SARS-CoV-2 Main Protease Non-Covalent Inhibitors: An In-Silico Study. *Int. J. Mol. Sci.* **2023**, *24*, 4237. https://doi.org/10.3390/ijms24044237.
9. Saied, E.M.; El-Maradny, Y.A.; Osman, A.A.; Darwish, A.M.G.; Abo Nahas, H.H.; Niedbała, G.; Piekutowska, M.; Abdel-Rahman, M.A.; Balbool, B.A.; Abdel-Azeem, A.M. A Comprehensive Review about the Molecular Structure of Severe Acute Respiratory Syndrome Coronavirus 2 (SARS-CoV-2): Insights into Natural Products against COVID-19. *Pharmaceutics* **2021**, *13*, 1759. https://doi.org/10.3390/pharmaceutics13111759.
10. Jin, Z.; Du, X.; Xu, Y.; Deng, Y.; Liu, M.; Zhao, Y.; Zhang, B.; Li, X.; Zhang, L.; Peng, C.; et al. Structure of M(pro) from SARS-CoV-2 and discovery of its inhibitors. *Nature* **2020**, *582*, 289–293. https://doi.org/10.1038/s41586-020-2223-y.
11. Dai, W.; Zhang, B.; Jiang, X.M.; Su, H.; Li, J.; Zhao, Y.; Xie, X.; Jin, Z.; Peng, J.; Liu, F.; et al. Structure-based design of antiviral drug candidates targeting the SARS-CoV-2 main protease. *Science* **2020**, *368*, 1331–1335. https://doi.org/10.1126/science.abb4489.
12. Tan, J.; George, S.; Kusov, Y.; Perbandt, M.; Anemüller, S.; Mesters, J.R.; Norder, H.; Coutard, B.; Lacroix, C.; Leyssen, P.; et al. 3C protease of enterovirus 68: Structure-based design of Michael acceptor inhibitors and their broad-spectrum antiviral effects against picornaviruses. *J. Virol.* **2013**, *87*, 4339–4351. https://doi.org/10.1128/jvi.01123-12.
13. Owen, D.R.; Allerton, C.M.N.; Anderson, A.S.; Aschenbrenner, L.; Avery, M.; Berritt, S.; Boras, B.; Cardin, R.D.; Carlo, A.; Coffman, K.J.; et al. An oral SARS-CoV-2 M(pro) inhibitor clinical candidate for the treatment of COVID-19. *Science* **2021**, *374*, 1586–1593. https://doi.org/10.1126/science.abl4784.
14. Fu, L.; Ye, F.; Feng, Y.; Yu, F.; Wang, Q.; Wu, Y.; Zhao, C.; Sun, H.; Huang, B.; Niu, P.; et al. Both Boceprevir and GC376 efficaciously inhibit SARS-CoV-2 by targeting its main protease. *Nat. Commun.* **2020**, *11*, 4417. https://doi.org/10.1038/s41467-020-18233-x.
15. Joyce, R.P.; Hu, V.W.; Wang, J. The history, mechanism, and perspectives of nirmatrelvir (PF-07321332): An orally bioavailable main protease inhibitor used in combination with ritonavir to reduce COVID-19-related hospitalizations. *Med. Chem. Res.* **2022**, *31*, 1637–1646. https://doi.org/10.1007/s00044-022-02951-6.
16. Bonatto, V.; Lameiro, R.F.; Rocho, F.R.; Lameira, J.; Leitão, A.; Montanari, C.A. Nitriles: An attractive approach to the development of covalent inhibitors. *RSC Med. Chem.* **2023**, *14*, 201–217. https://doi.org/10.1039/d2md00204c.
17. Cotrim, B.A.; Barros, J.C. Development and patent synthesis of nirmatrelvir–the main component of the first oral drug against SARS-CoV-2 Paxlovid®. *Aust. J. Chem.* **2022**, *75*, 487–491.
18. Jiang, B.; Li, G.; Yu, J.; Xu, X.; Pan, H.; Zhao, C.; Zhong, J.; Zhang, F. Synthesis and crystal characteristics of nirmatrelvir. *React. Chem. Eng.* **2023**, *8*, 1747–1759. https://doi.org/10.1039/D3RE00019B.
19. Algera, R.F.; Allais, C.; Baldwin, A.F.; Becirovic, H.; Bowles, P.; Brown, A.R.; Buske, J.M.; Clarke, H.J.; Do, N.M.; Doyle, K.; et al. Synthesis of Nirmatrelvir: Development of an Efficient, Scalable Process to Generate the Western Fragment. *Org. Process Res. Dev.* **2023**, *27*, 2240–2249. https://doi.org/10.1021/acs.oprd.3c00249.
20. Algera, R.F.; Allais, C.; Becirovic, H.; Brown, A.R.; Chen, B.; Clarke, H.J.; Concannon, P.E.; Du, Y.; Georgian, W.; Lee, J.W.; et al. Synthesis of Nirmatrelvir: Development of Magnesium Sulfate-Mediated Aminolysis for the Manufacture of the Eastern Fragment. *Org. Process Res. Dev.* **2023**, *27*, 2271–2279. https://doi.org/10.1021/acs.oprd.3c00252.

21. Algera, R.F.; Allais, C.; Baldwin, A.F.; Busch, T.; Colombo, F.; Colombo, M.; Depretz, C.; Dumond, Y.R.; Faria Quintero, A.R.; Heredia, M.; et al. Synthesis of Nirmatrelvir: Development of a Scalable Cobalt-Catalyzed Cyclopropanation for Manufacture of the Bicyclic [3.1.0] Proline-Building Block. *Org. Process Res. Dev.* **2023**, *27*, 2260–2270. https://doi.org/10.1021/acs.oprd.3c00251.
22. Werth, J.; Uyeda, C. Cobalt-Catalyzed Reductive Dimethylcyclopropanation of 1,3-Dienes. *Angew. Chem. Int. Ed. Engl.* **2018**, *57*, 13902–13906. https://doi.org/10.1002/anie.201807542.
23. Porta, R.; Benaglia, M.; Puglisi, A. Flow Chemistry: Recent Developments in the Synthesis of Pharmaceutical Products. *Org. Process Res. Dev.* **2016**, *20*, 2–25. https://doi.org/10.1021/acs.oprd.5b00325.
24. Preschel, H.D.; Otte, R.T.; Zhuo, Y.; Ruscoe, R.E.; Burke, A.J.; Kellerhals, R.; Horst, B.; Hennig, S.; Janssen, E.; Green, A.P.; et al. Multicomponent Synthesis of the SARS-CoV-2 Main Protease Inhibitor Nirmatrelvir. *J. Org. Chem.* **2023**, *88*, 12565–12571. https://doi.org/10.1021/acs.joc.3c01274.
25. Kincaid, J.R.A.; Caravez, J.C.; Iyer, K.S.; Kavthe, R.D.; Fleck, N.; Aue, D.H.; Lipshutz, B.H. A sustainable synthesis of the SARS-CoV-2 M(pro) inhibitor nirmatrelvir, the active ingredient in Paxlovid. *Commun. Chem.* **2022**, *5*, 156. https://doi.org/10.1038/s42004-022-00758-5.
26. Okabe, H.; Naraoka, A.; Isogawa, T.; Oishi, S.; Naka, H. Acceptor-Controlled Transfer Dehydration of Amides to Nitriles. *Org. Lett.* **2019**, *21*, 4767–4770. https://doi.org/10.1021/acs.orglett.9b01657.
27. Wood, A.B.; Kincaid, J.R.A.; Lipshutz, B.H. Dehydration of primary amides to nitriles in water. Late-stage functionalization and 1-pot multistep chemoenzymatic processes under micellar catalysis conditions. *Green Chem.* **2022**, *24*, 2853–2858. https://doi.org/10.1039/D1GC04671C.
28. Caravez, J.C.; Iyer, K.S.; Kavthe, R.D.; Kincaid, J.R.A.; Lipshutz, B.H. A 1-Pot Synthesis of the SARS-CoV-2 Mpro Inhibitor Nirmatrelvir, the Key Ingredient in Paxlovid. *Org. Lett.* **2022**, *24*, 9049–9053. https://doi.org/10.1021/acs.orglett.2c03683.
29. Shanahan, C.S.; Kadam, A.L.; Chiranjeevi, B.; Nunes, A.A.; Jayaraman, A.; Ahmad, S.; Aleshire, S.L.; Donsbach, K.O.; Gupton, B.F.; Nuckols, M.C. Efforts to develop a cost-effective and scalable synthetic process for nirmatrelvir. *ChemRxiv* **2022**. https://doi.org/10.26434/chemrxiv-2022-cn0k1.
30. Algera, R.F.; Baldwin, A.F.; Bowles, P.; Clarke, H.J.; Connor, C.G.; Cordi, E.M.; Do, N.M.; Nicholson, L.D.; Georgian, W.; Happe, A.; et al. Synthesis of Nirmatrelvir: Design and Optimization of an Efficient Telescoped Amidation–Dehydration Sequence. *Org. Process Res. Dev.* **2023**, *27*, 2250–2259. https://doi.org/10.1021/acs.oprd.3c00250.
31. Hu, Y.N.; Lewandowski, E.M.; Tan, H.; Zhang, X.; Morgan, R.T.; Zhang, X.; Jacobs, L.M.C.; Butler, S.G.; Gongora, M.V.; Choy, J.; et al. Naturally Occurring Mutations of SARS-CoV-2 Main Protease Confer Drug Resistance to Nirmatrelvir. *ACS Cent. Sci.* **2023**, *9*, 1658–1669.
32. Dayan Elshan, N.G.R.; Wolff, K.C.; Riva, L.; Woods, A.K.; Grabovyi, G.; Wilson, K.; Pedroarena, J.; Ghorai, S.; Nazarian, A.; Weiss, F.; et al. Discovery of CMX990: A Potent SARS-CoV-2 3CL Protease Inhibitor Bearing a Novel Warhead. *J. Med. Chem.* **2024**, *67*, 2369–2378. https://doi.org/10.1021/acs.jmedchem.3c01938.
33. Ghosh, A.K.; Yadav, M.; Iddum, S.; Ghazi, S.; Lendy, E.K.; Jayashankar, U.; Beechboard, S.N.; Takamatsu, Y.; Hattori, S.I.; Aamano, M.; et al. Exploration of P1 and P4 modifications of nirmatrelvir: Design, synthesis, biological evaluation, and X-ray structural studies of SARS-CoV-2 Mpro inhibitors. *Eur. J. Med. Chem.* **2024**, *267*, 116132. https://doi.org/10.1016/j.ejmech.2024.116132.
34. Brewitz, L.; Dumjahn, L.; Zhao, Y.; Owen, C.D.; Laidlaw, S.M.; Malla, T.R.; Nguyen, D.; Lukacik, P.; Salah, E.; Crawshaw, A.D.; et al. Alkyne Derivatives of SARS-CoV-2 Main Protease Inhibitors Including Nirmatrelvir Inhibit by Reacting Covalently with the Nucleophilic Cysteine. *J. Med. Chem.* **2023**, *66*, 2663–2680. https://doi.org/10.1021/acs.jmedchem.2c01627.